

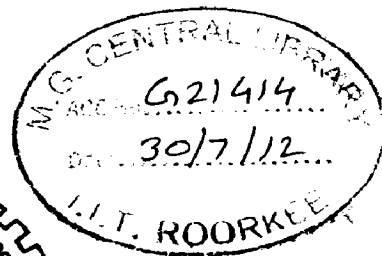
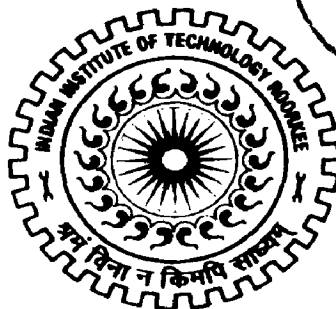
INVERSION OF 2D MAGNETOTELLURIC DATA USING MT2DINVMATLAB

A DISSERTATION

*Submitted in partial fulfillment of the
requirements for the award of the degree*
of
MASTER OF TECHNOLOGY
in
GEOPHYSICAL TECHNOLOGY

By

SHIVENDRA KUMAR YADAV



**DEPARTMENT OF EARTH SCIENCES
INDIAN INSTITUTE OF TECHNOLOGY ROORKEE
ROORKEE - 247 667 (INDIA)
JUNE, 2012**

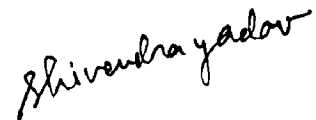
CANDIDATE'S DECLARATION

I hereby declare that the work which is being presented in this dissertation, entitled '**Inversion of 2D Magnetotelluric data using MT2DInvMatlab**' in the partial fulfillment of the requirement for the award of **Master of Technology in Geophysical Technology** submitted in **Department of Earth Sciences, Indian Institute of Technology, Roorkee**, carried out during a period of July 2011 to May 2012 under the supervision of **Dr. M. Israil**, Professor, Department of the Earth Sciences, Indian Institute of Technology, Roorkee.

The matter embodied in this dissertation has not been submitted by me for the award of any other degree.

Dated: 5/06/2012

Place: IIT ROORKEE



Shivendra Kumar Yadav

This is to certify that the above statement made by the candidate is correct to the best of my knowledge.



Dr. M. Israil
Professor

Department of Earth Sciences
Indian Institute of Technology,
Roorkee-India

ACKNOWLEDGEMENT

This dissertation is the result of my last year work whereby I have been helped and supported by many people. It's a matter of great pleasure to acknowledge the help I have had in completing the dissertation work.

First, I want to express my special gratitude to my supervisors Prof. M. Israil. I specially thank to Prof. M. Israil for taking maximum responsibility in guiding me for my thesis write up. I am indebted to him for giving me the opportunity to carry out field work. He always encouraged me during work and motivate to ask good questions to help me think through my problems.

I am very thankful to Prof. H. Sinvhal to give me opportunity to present my work.

I am grateful to Prof P. K. Gupta and Prof A. K. Saraf for providing necessary facilities during their respective periods as the Head of the Department. I would like to make a special note of thanks to Dr. Elena Sokolova (GEMRI), Dr. Dimitri, and Anna Ilyina. I am grateful to Dr. Seong Kong L, Hee Joon Kim, Yoonho Song, and Choon-Ki Lee (Korea Institute of geoscience and Mineral Resources, Republic of Korea), for providing their MT2DInvMatlab code on internet.

I offer my special thanks to Mr. Manoj Kumar Rout, Mr. Suresh Kanaujiya, Mr. Sonu Kumar and other colleagues for their help in field work. I am grateful to the technical and non-technical staff of Department of Earth Sciences, IIT Roorkee for their cooperation and helpful behaviour.

(Shivendra Kumar Yadav)

ABSTRACT

Magnetotelluric method gives information of electric property of subsurface at deeper depth and it is also cheaper. Study area of this work is Roorkee-Gangotri region which lies in Himalaya. Himalaya has very interesting geological structure and features. Recent year's magnetotelluric method is using to explore new information about it.

In the present thesis, I have used, MT2DInvMatlab, a 2D inversion programe to invert MT data from Himalayan region.

In this dissertation, magnetotelluric data were acquired using Phoenix system at 7 stations. Phoenix data processed with software (PRC-MTMV and SSMT 2000) based on multi-level robust averaging scheme. Other 35 station data recorded by metronics system (Israil et al, 2008) were added. Total 42 station data were averaged to 18 station data of good quality. Inversion of these 18 station data was done by MT2DInvMatlab programe to conclude the information about subsurface of Roorkee-Gangotri region. Inverted resistive section shows different electrical structure beneath Roorkee-Gangotri region. It shows shallow conductive sediments between Indo-Gangetic Plane and Lesser Himalaya, and high resistivity top of Indian crust. It also depicts a conducting zone might be related with the strain accumulation zone in Himalayan region.

CONTENT

List of Figures	v
List of Tables	vii
CHAPTER 1 INTRODUCTION	1
1.1 Overview of magnetotelluric method	1
1.2 Magnetotelluric Signal generation	2
1.3 Basic Theory of Magnetotelluric	3
1.3.1 Transfer operators	5
1.4 Other Terms	6
1.4.1 Coherency	6
1.4.2 Pseudo Section	7
1.4.3 EDI File	7
CHAPTER 2 DATA ACQUISITION	9
2.1 MT Site Deployment	9
2.1.1 Study Area	9
2.1.2 Site Selection	11
2.1.3 Instrument description and deployment	11
2.1.3.1 Data Logger	12
2.1.3.2 Electric and Magnetic Sensor	13
2.1.3.3 Battery, GPS and Wires	14
2.1.3.4 Accessories	14
2.2 Data Acquisition: Phoenix System	15
2.2.1 Phoenix V5 System	15
2.2.2 Data Recording	16
2.2.2.1 Calibration	16
2.2.2.2 Acquisition Parameter setting	16
CHAPTER 3 DATA PROCESSING	22
3.1 Theory of PRC-MTMV	22
3.1.1 Pre-processing and Spectral Analysis	23
3.1.2 Transfer Functions Estimation for single segment	24

3.1.3	Averaging of Transfer Operators over set of partial estimates	25
3.1.4	Averaging over multi-window	27
3.1.5	Multi-RR Estimation	27
3.1.6	Estimating Geomagnetic Transfer Functions	28
3.2	Field Data Processing: Phoenix Time series	28
3.2.1	SSMT 2000 Processing	28
3.2.2	PRC-MTMV Processing	32
3.3	Flowcharts	39
3.3.1	SSMT Processing Flowchart	39
3.3.2	PRC-MTMV Processing Flowchart	40
CHAPTER 4	2D INVERSION THEORY: MT2DInvMatlab	41
4.1	MT2DInvMatlab Theory	41
4.1.1	Forward modeling	41
4.1.2	Least squares Inversion	44
4.2	Files Description	45
4.2.1	Parameter script file (*.m)	45
4.2.2	Field Data File (*.FDT)	46
4.2.3	Topography File (*.TOP)	46
4.2.4	Output MT inversion file (*.MIR)	46
4.3	Data Editing	46
CHAPTER 5	RESULTS AND DISCUSSION	50
5.1	Inversion of field data	50
5.2	Results and Discussion	51
CHAPTER 6	SUMMARY AND CONCLUSION	66
	REFERENCE	67

List of Figures

Figure 1.1	Earth's magnetosphere	2
Figure 2.1	Map of MT stations	10
Figure 2.2	Standard MT site layout	11
Figure 2.3	Magnetic Sensor and Phoenix data logger	12
Figure 2.4	WinTabEd main Window	17
Figure 2.5	LED Pattern for Phoenix data acquisition	19
Figure 2.6	Time span of Phoenix Data	21
Figure 3.1	Main window of SSMT 2000	28
Figure 3.2	Window of setting for *.PFT file	29
Figure 3.3	Window of setting for *.PRM file	30
Figure 3.4	Apparent resistivity and phase plot for base-3 station using MT-PLOT	32
Figure 3.5	Screenshot of *.CHN file	33
Figure 3.6	Screenshot of *.PRC file	33
Figure 3.7	Main window of PRC-MTMV	34
Figure 3.8	Visualisation of time series in PRC-MTMV	35
Figure 3.9	Amplitude and Phase plot of transfer operator in PRC-MTMV	35
Figure 3.10	Plot of apparent resistivity for point-3 station	37
Figure 3.11	Plot of apparent phase for point-3 station	38
Figure 4.1	Plot of averaged apparent resistivity and phase for group 1	48
Figure 4.2	Map of 18 Station	49
Figure 5.1	Pseudo Section of apparent resistivity and phase	
Figure 5.1.1	TM Mode	52
Figure 5.1.2	TE Mode	53

Figure 5.2	Models for TE and TM mode inversion	
Figure 5.2.1	Model for TM Mode	54
Figure 5.2.2	Model for TE Mode	55
Figure 5.2.3	Model by Israil et al., 2008	55
Figure 5.3	Fitting plot for TM Mode	
Figure 5.3.1	Resistivity fitting plot for TM mode	56
Figure 5.3.2	Phase fitting plot for TM mode	58
Figure 5.4	Fitting plot for TE Mode	
Figure 5.4.1	Resistivity fitting plot for TE mode	60
Figure 5.4.2	Phase fitting plot for TE mode	62

List of Tables

Table 2.1 MT Survey Equipment Checklist	14
Table 2.2 Phoenix Station details	20
Table 3.1 Spectral window sequence detail	36
Table 4.1 List of averaged Stations and corresponding reference Station	47

CHAPTER 1

INTRODUCTION

1.1 Overview of Magnetotelluric Method

Magnetotelluric method is an advanced electromagnetic method that uses natural variations in the Earth's magnetic field as a source. Frequency range of earth's natural magnetic field varies in very vast range, thus giving opportunity to study the resistive property of subsurface of the earth to deeper depths. The large frequency range also means that the method is not hampered by the presence of conductive overburden or sampling frequencies that do not allow for deep penetration (Kaufman and Keller, 1981).

A major advantage of the MT method is that it simultaneously measures the electric and magnetic fields in two perpendicular directions. This provides useful information about electrical anisotropy in an area. Other advantages include the wide frequency range at which data can be sampled. It is also cheaper than for example deep reflection seismic surveys (Vozoff et al., 1975).

The basic assumption of magnetotelluric method is that the source is a natural electromagnetic plane wave propagating in vertical direction and earth medium in which it propagates have layered structure (Christoffel et al., 1968).

If frequencies of measured magnetotelluric signal lie in range of audio-frequencies (1 to 10^5 Hz), then this particular method is called as audio-magnetotelluric method (AMT). Similarly another magnetotelluric method is Controlled Source Audio-Magnetotelluric (CSAMT) which is a frequency-domain EM sounding technique with artificial source. Grounded dipole or horizontal loop used as an artificial source. The use of an artificial signal source is the main difference between the CSAMT and MT methods. The artificial source in CSAMT provides a stable, dependable signal, resulting in higher-precision and more economical measurements than are usually obtainable with natural source measurements in the same bandwidth. Application of CSAMT and AMT is to map groundwater, base metal deposits and geothermal resources at depths from 50-100 m to several kilometers (Zonge et al., 1991). MT method becomes a very successful method in those areas where reflection seismology method becomes failed or very expensive like in extreme terrain and beneath volcanic.

Noise is the very big problem in magnetotelluric method. Magnetotelluric signal are very noise sensitive. There are two type noises: Man made noises and Natural noises.

Man-made electrical noise, such as power lines, power generators, and moving vehicles and trains, can affect MT data quality very badly. All of these local disturbances produce incoherent noise that mainly affects frequencies above 1 Hz.

Local lightning, wind, and rainstorms are natural noises which also reduce the data quality. There are many precautions which should follow from site selection to site deployment, so we can reduce considerable amount of noise. These precautions like site should be far distance from power-lines, telephone wires, railway tracks, or industry. During site deployments, magnetic induction coils and the electric dipole wires should covered by soil, which minimized wind noise. Noises generated from small power lines and moving vehicles becomes negligible at distances greater than 0.4 km. Noise from larger power lines, power generators, pipelines, and trains was negligible at distances greater than 5 km (Simpson and Bahr, 2005).

1.2 Magnetotelluric Signal generation

Natural MT signals come from a variety of sources, but in the frequency range of interest ($\sim 0.001\text{--}10^4$ Hz), the atmosphere and magnetosphere are the main source regions. The higher frequency component mainly emanates from meteorological activities such as lightning. In higher range of frequency, electromagnetic field was generated by thunderstorms. It occurs mainly in equatorial regions (Christopherson, 1998).

Variations in the Earth's magnetic field linked to solar activity are responsible for a low frequency field. Micropulsation is the major phenomenon for generation of low frequency signal. These fields arise from complex interaction of charged particle in the solar wind with the earth's magnetic field and charged particles in the ionosphere (Jacobs et al., 1964). Signal generated by this phenomenon can vary in magnitude on daily, weekly or yearly basis. So during data recording this can increase noise in recorded signal. So in acquisition planning, solar forecast can play important role.

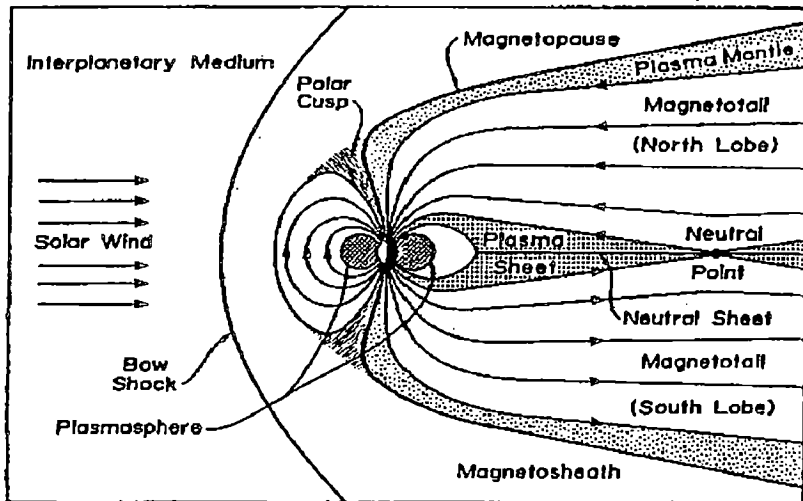


Figure 1.1: Earth's magnetosphere
 (Akasofu S. I. and Kamide Y., "The Solar Wind and the Earth", Tokyo, 1987, pp. 73-100)

1.3 Basic theory of Magnetotelluric

Electromagnetic wave motion is governed by following four Maxwell equations. Assuming a polarized and magnetized medium containing no electric and magnetic sources, Maxwell equation can be written as:

$$\nabla \cdot B = 0 \quad 1.1.1$$

$$\nabla \cdot D = \rho \quad 1.1.2$$

$$\nabla \times E = -\frac{\partial B}{\partial t} \quad 1.1.3$$

$$\nabla \times H = j + \frac{\partial D}{\partial t} \quad 1.1.4$$

However, in the presence of a linear, isotropic medium the material equations can be introduced

$$B = \mu H \quad 1.2.1$$

$$D = \epsilon E \quad 1.2.2$$

And current density in any conductor of conductivity σ in presence of electric field E is given by Ohm's law:

$$J = \sigma E \quad 1.3$$

Using above equations $B = \mu H, D = \epsilon E$ and Ohm's law, the Maxwell equations can be written as:

$$\nabla \cdot B = 0 \quad 1.4.1$$

$$\nabla \cdot D = \frac{\rho}{\epsilon} \quad 1.4.2$$

$$\nabla \times E = -\frac{\partial B}{\partial t} \quad 1.4.3$$

$$\nabla \times H = \mu \sigma E + \mu \epsilon \frac{\partial E}{\partial t} \quad 1.4.4$$

Using above equations we can derive following wave equation for source free region which govern the magnetotelluric signal.

$$\nabla^2 V - k^2 V = 0 \quad 1.5$$

Where V will be magnetic field H or Electric field E, and k is propagation vector given by

$$k^2 = i\omega\mu\sigma - \omega^2\mu\epsilon \quad 1.6$$

At very low frequency, depth of penetration of magnetotelluric signal can be given by only first term $i\omega\mu\sigma$, which describe the diffusion of EM signal. On the basis of depth penetration term **skin depth** defined as the distance by which the amplitude of signal decay up to 1/e of surface value of amplitude. Skin depth in any medium is given by

$$\delta(\omega) = \sqrt{\frac{2}{\omega\mu\sigma}} \quad (\text{In meter}) \quad 1.7$$

In case, length of geological structure is large in comparison of width then it can consider as 2D body. In 2D case, MT equations divide in to two mode of propagation. In one mode, electric signal is parallel to the strike of geological structure called TE Mode. In second mode, electric current is perpendicular to structure which refer as TM Mode (Kaufman and Keller, 1981).

1.3.1 Transfer operators

In measurement of magnetotelluric signal, we record two components of electric field E_x and E_y , and three component of magnetic field H_x , H_y , and H_z . Transfer operators are the ratio of MT signals. **Horizontal magnetic tensor M** relates two horizontal magnetic fields. **Tipper S_z** relates vertical magnetic field to horizontal magnetic field. **Telluric operator T** relates horizontal electric field (Varentsov et al., 2002). **Impedance tensor Z** is most important transfer operator which is ratio of electric field to magnetic field (Cagniard, 1953). Impedance tensor Z can be written as:

$$Z(\omega) = \frac{E(\omega)}{H(\omega)} \quad 1.8$$

Where

$$E(\omega) = \begin{bmatrix} E_x(\omega) \\ E_y(\omega) \end{bmatrix}, H(\omega) = \begin{bmatrix} H_x(\omega) \\ H_y(\omega) \end{bmatrix}, \quad 1.9$$

$$Z(\omega) = \begin{bmatrix} Z_{xx}(\omega) & Z_{xy}(\omega) \\ Z_{yx}(\omega) & Z_{yy}(\omega) \end{bmatrix} \quad 1.10$$

Equation expands as following equation:

$$E_x(\omega) = Z_{xx}(\omega)H_x(\omega) + Z_{xy}(\omega)H_y(\omega) \quad 1.11.1$$

$$E_y(\omega) = Z_{yx}(\omega)H_x(\omega) + Z_{yy}(\omega)H_y(\omega) \quad 1.11.2$$

Similarly, the magnetic transfer function can be written as,

$$H_z = T_{zx}H_x + T_{zy}H_y \quad 1.12$$

Here Z_{xx} , Z_{xy} , Z_{yx} , Z_{yy} and T_{zx} , T_{zy} may be a complex numbers and these are functions of frequency, electrical properties of medium, orientation of measurement axes and location of the observation site.

For 1D structure (layered model), the amplitude of off diagonal elements of impedance tensor are equal and diagonal elements are zero. The impedance tensor will be scalar.

$$Z_{xy} = -Z_{yx} = |Z| \text{ and } Z_{xx} = Z_{yy} = 0 \quad 1.13$$

For a 2D earth, and TE and TM mode, the diagonal elements becomes zero and the off diagonal elements are different,

$$Z_{xx} = Z_{yy} = 0 \text{ and } Z_{xy} = Z_{yx} \neq 0 \quad 1.14$$

Impedance normally represent in form amplitude and phase. Phase of Impedance tensor given by

$$\varphi_{ij} = \tan^{-1} \left(\frac{\text{Im}(Z_{ij})}{\text{Re}(Z_{ij})} \right) \quad 1.15$$

Resistivity obtained from the impedance is called “apparent” resistivity, which is frequency dependent. The apparent resistivity ρ_{aij} [Ωm] ($i, j = x, y$) in terms of the impedance tensor is given by:

$$\rho_{aij}(\omega) = \frac{1}{\mu_0 \omega} |Z_{ij}(\omega)|^2 \quad 1.16$$

In homogeneous medium, apparent resistivity will be true resistivity.

In a homogenous earth the impedance phase is (45°). In a 1D-layered Earth, when MT signal propagate through higher conductive media phase increases over 45° . In similar manner, phase reduced below 45° for the EM response penetrating into a less conducting media (Kaufman and Keller, 1981).

1.4 Other Important Terms

1.4.1 Coherency

Coherency is a measure of the signal-to-noise ratio of the vertical magnetic field with respect to each of the orthogonal, horizontal magnetic field directions. Values are normalized between 0 and 1. Coherency is used for checking of data quality. For two signals A and B then coherency between A and B is given as:

$$coh_{AB} = \frac{AB^*}{\sqrt{AA^* BB^*}} \quad 1.17$$

Here A and B both may be $E_x, E_y, H_x, H_y,$ and H_z (Jones, 2002).

1.4.2 Pseudo Sections

The Pseudo-Sections are the surface plot of any measuring parameter values on 2D graph where one axes is frequency and other one is distance of each station along a profile. Here values of parameter are interpolated for different frequency and distance. Parameter values are shown by different color. In magnetotelluric case, apparent resistivity, apparent phase and tipper values are displayed as pseudo-sections to see their behavior against frequency and distance.

1.4.3 EDI File

EDI (Electrical Data Interchange) file is a standard format file, which adapted for interchanging of magnetotelluric data, or similar electrical geophysical data. It is designed in such format that archival and interchange of data became very convenience. It is not designed for a working purpose. Format of EDI file is corresponding to source code file for any computer program it used as source code file. EDI files are ASCII text files (Wieght, 1988).

It used as input file in many software. Almost every software give facility to convert their specific into EDI file.

EDI files are formed by different Data Blocks, sometimes it simply called Blocks. Each data blocks contain a keyword, and followed by one or more **options**, and then followed by data set, if it is there (Wieght, 1988).

Each data blocks start with a keyword. A keyword always start with the identifier '>' character. Examples of keywords are >HEAD, >SPECTRA, >FREQ, >ZXXR, >ZROT etc. More than 100 keywords are defined for EDI files. An option has two parts: an option name, and an option argument, which parted by an equal sign (=). Examples of options are:

```
DATAID="poin11-t-1r"  
ACQBY="MSU-Geophysics"  
FILEBY="Pushkarev"  
ACQDATE=10/10/11  
FILEDATE=2011/12/24  
COUNTRY="India"  
STATE="Narkatiaganj"  
LAT=29:49:0  
LONG=77:49:50
```

ELEV=240

A data set start with keyword, which defined for that data type, then followed by two slash characters //, then followed by a number which gives the number of data values. Then from next row, data values are followed. Each row of data value contains five columns. Generally data values are presented in float format. An EDI file is a sequence of data blocks. Every data block have exact same format that described above (Wieght, 1988).

Number of sequences of data blocks can be collectively form one section depending on data type. For example different component of impedance tensor form different data block and collectively they form one section of impedance tensor. There are many sections in EDI file like apparent resistivity, Impedance phase etc. Each section start with a special data block whose keyword is a two characters >=. EDI file finish with >END block after all of the data sections are presented (Wieght, 1988).

CHAPTER 2

DATA ACQUISITION

Magnetotelluric data comprises natural time-varying orthogonal components of the horizontal electric field ($E_x(t), E_y(t)$) and of the magnetic field ($B_x(t), B_y(t), B_z(t)$), recorded simultaneously on the earth surface. Number of instruments is available to measure the time varying components of the earth's natural electromagnetic field. These instruments are able to record field components in the desired frequency range with high sensitivity, accuracy and resolution. Magnetotelluric data recorded along Roorkee-Gangotri profile used in my dissertation work, these data were recorded by two different types of system, Metronics system and Phoenix V5 system. All Metronics station data along profile has recorded earlier by Prof. M. Israil and his group (Israil et al, 2008) in 2004-06. During 13th October, 2011 to 24th October, 2011, phoenix system deployed at various stations to record magnetotelluric data. Phoenix data were recorded under Indo-Russian joint project. During this data recording, I participate first 10 days with the group of other students: Manoj Kumar Rout, Suresh Kanaujiya and Sonu Kumar.

2.1 MT Site Deployment

I have processed a few stations phoenix data in my dissertation work. In this chapter, I shall discuss the phoenix system, its deployment, recording parameter and time series format. MT site deployment is a very rigorous work and required careful attention with experience, because quality of data depends on each and every small step.

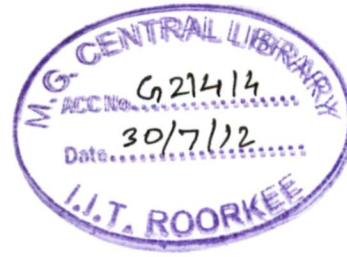
2.1.1 Study Area

I used 42 stations MT data in my dissertation work in which 7 station data are recorded by phoenix system and other 35 station data were taken from Prof. M.Israil (Israil et al, 2008). All data are lie along the profile Roorkee-Gangotri, which clearly indicate my study area lie between Indo Gangetic plane and Higher Himalay. Among these 42 station data, some are averaged to remove cluster of station, then processed and finally 18 station data were used as input data for inversion program. Length of profile is approximately 170 km.

Roorkee-Gangotri region lies under Himalaya region and have interesting geology. Himalaya mountain series is result of collision between Indian and Eurasian plate 50-40

million years. Due to this collision many geological structural formed. Himalayan region is divided into following four zones:

1. Siwalik Himalayas or Sub-Himalaya
2. Lower or Lesser Himalaya
3. Central or Higher Himalaya
4. Trans or Tethyan Himalaya



Siwalik Himalaya and Indo-Gangetic plane separate by MFT (Main Frontal Thrust), Siwalik and Lower Himalaya divided by MBT (Main Boundary Thrust), Lower and Higher Himalaya are separated by MCT (Main Central Thrust), and ITS (Indian Tsangpo Suture) is boundary where Indian and Eurasian collide. Geographic map of Roorkee-Gangotri profile along with station location is shown in figure (2.1). This figure is generated by GMT software with the help Mr. Suresh Kanaujiya.

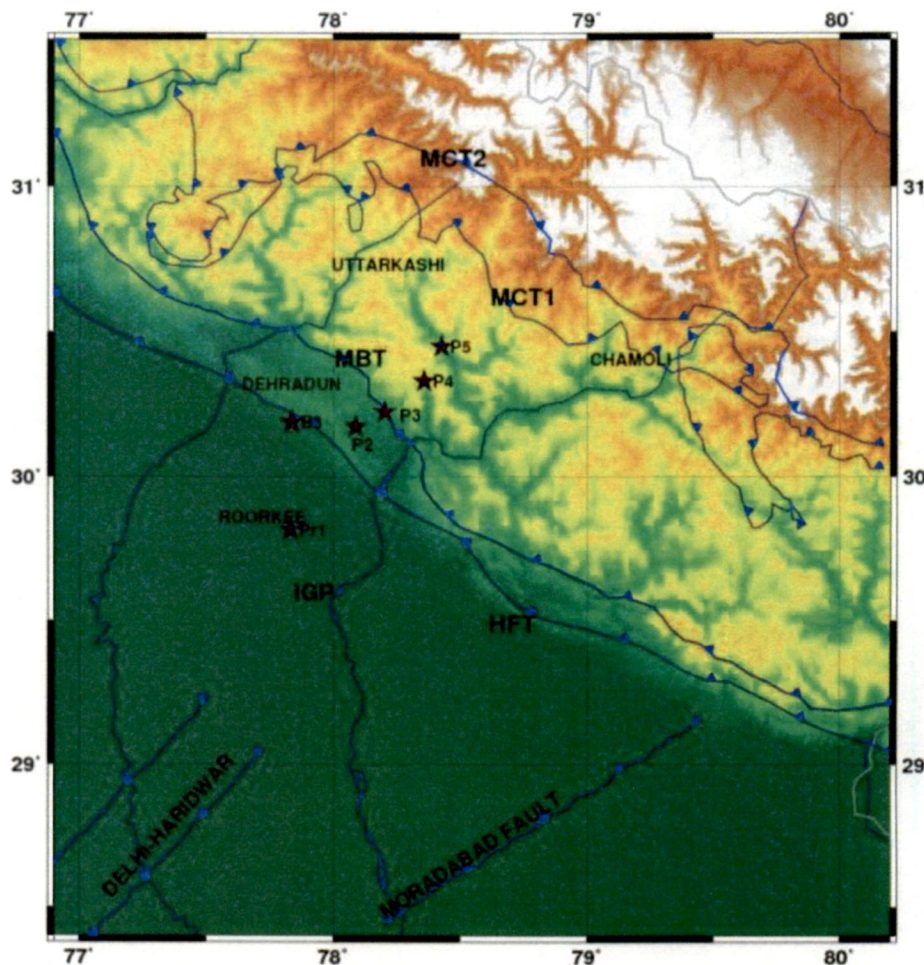


Figure 2.1: Map of MT stations

2.1.2 Site Selection

Site selection is very important because site which is not carefully chosen with precaution can result very noisy and useless data. We should take care of each and every restriction like:

- Site should be sufficient away from power-line and Railway tracks,
- Should be electrically quiet place,
- Sufficient area should be available for deployment of instrument with no obstacle,
- if available then it should be planar, otherwise slope should less than 20° ,
- Make sure profile is straight; stations are not more divergent from profile line.

2.1.3 Instrument description and deployment

After selection of proper site, first make checklist (Table 2.1) that you have brought every instrument and equipment which would be necessary in deployment. After checking, start deployment.

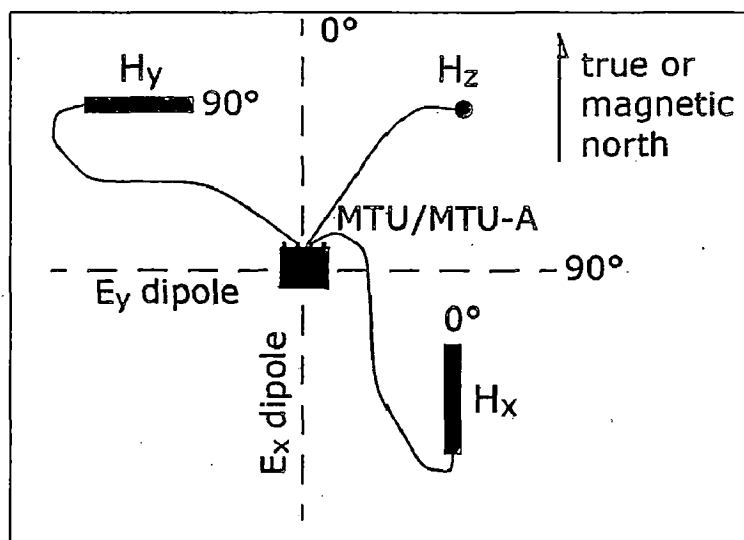


Figure 2.2: Standard MT site layout
(V5 System 2000 MTU/MTU-A User Guide, Version 1.6, September 2005)

For any MT system arrangement and deployment is same. Arrangement of deployment is as figure (2.2), where four electric sensors make two perpendicular dipole and recording instrument is at centre. Three Magnetic coils, for H_x , H_y and H_z , are deployed at different quadrature formed by two dipoles. Two coils corresponding to H_x and H_y should be buried in

soil elongated in direction of N-S and E-W respectively. These coils should be horizontal. Third coil buried in deep hole vertically. After deploying electric and magnetic sensor, spread wires and cable to make connection between sensors and Data logger.

2.1.3.1 Data Logger

Data logger is equipment where each magnetic and electrical sensor, battery, and GPS is connected by wires and cables. It is placed at center of MT site. After making connection, we can check in data logger that everything (like wire connection, battery status, GPS) is OK or not. Setting for acquisition parameter, calibration of instrument and sensor should be done in the beginning of survey.

The instruments can record maximum two component of electric field, and three components of magnetic data from coil sensors. The instruments synchronize to Co-ordinated Universal Time (UTC) via signals from Global Positioning System (GPS) satellites. The GPS synchronization means that sites even very remote from the survey can be used to acquire low noise reference data, vastly improving the quality and reliability of the survey results (MTU User Guide 1.6, 2005).

Brief description of Phoenix systems, setting and procedure of handling is described in section 2.2.



Figure 2.3: Magnetic Sensor and Phoenix data logger

2.1.3.2 Electric and Magnetic Sensor

Each electric sensor consists of lead-chloride porous pot electrodes buried about 25cm deep in salty mud, connected to the recording system by cables (commonly called E-lines). The dipoles form a right angle cross, with the center.

Typically, length of E-line is from 25 to 100m long, making dipole length 50 to 200m long. Signal-to-noise ratio increases with dipole length but the greater the AC voltage induced by the local power grid. The north-south dipole is referred to as E_x and the east-west dipole is referred to as E_y . Similarly if E_x could not align in true north then rotate the E line, but enter this azimuth during processing. If site is not horizontal then E-lines will be inclined. If inclination is more than 20° , then use trigonometry to calculate true length of E-line. Excess cable should lay in elongated S-shapes and 5m away from both ends. It can distort signal by induction if these extra cable make close loop (MTU User Guide 1.6, 2005).

In general, the lower the contact resistance, the better. High contact resistance ($\geq 2000\Omega$), use following precaution:

- Lift the electrode
- Move the electrode to a new hole
- Replace the dirt in the hole with a mixture of salt water and either Bentonite

Magnetic sensor is used to measure the variation of magnetic field. It contains loop of copper wire wound into a high-permeability core. The response of the induction coil is governed by the rate of change of magnetic flux ($\partial\vec{B}/\partial t$) within the coil. Magnetometer of Metronix system is MFS06 and Phoenix system is MTC-50.

Each sensor should place in a different quadrant formed by the dipoles, as far from the Data logger as the connecting cable allows. Two magnetic sensors are placed horizontally for H_x and H_y , and one vertically for H_z . Sensor must be separated 5 m from instruments. The horizontal coils are normally aligned with the telluric dipoles, as carefully oriented and level as possible, buried in shallow depth. The coil placed with its free end pointing north is referred to as H_x . The coil with its free end pointing east is H_y . The third coil, H_z , should be set as precisely vertical as possible in a deep hole enough that the entire coil can be buried. This vertical coil is the sensor most susceptible to electrical coupling with the E-lines. In all cases, serial numbers of the coils must be noted down before burying them, and record on the layout Sheet which sensor is used as H_x , H_y , and H_z (MTU User Guide 1.6, 2005).

2.1.3.3 Battery, GPS and Wires

The instruments synchronize to Co-ordinated Universal Time (UTC) via signals from Global Positioning System (GPS) satellites. It is important at this stage to verify that the instrument has acquired "GPS lock". Data acquisition cannot begin unless GPS lock has been achieved (MTU User Guide 1.6, 2005).

Battery should be fully charged and should show 12.75 V on full charging. If data acquisition is made for many days then keep changing and charging regularly. Battery status can be shown in recording instrument. Figure (2.5) show two LED pattern: Normal pattern and Alternate pattern. If battery condition is OK then it follows normal pattern otherwise it follows Alternate pattern. In Alternate pattern, when something is wrong then it blinks rapidly for 350ms as a warning and then flashes from 1 to 7 times. 1 Number of flashes represents low battery (MTU User Guide 1.6 manual).

Wire and cables are spread to make connection between GPS, Battery and sensor to recording system. So check each wire is connected properly. Connect them carefully as given in manual/user guide of system. After installing MT site, cover spread wire and cables by soil.

2.1.3.4 Accessories

Other than above instruments, there are several things which need during installation of MT site. So use a checklist shown in table (2.1) to not forget anything. First column of table shows all essential components required in site deployment.

Table 2.1: MT Survey Equipment Checklist

(V5 System 2000 MTU/MTU-A User Guide, Version 1.6, September 2005)

S.No.	Instrument	Components ID Number (if required)	Number of items
1	MTU Box		
2	Flash Memory		
3	Battery		
4	Battery Cable		
5	GPS Antenna		
6	GPS cable		
7	Pot		
8	Sensor		

9	Airloop		
10	Sensor cable		
11	3-way Sensor connector		
12	E-line cable		
13	Ground pot cable		
14	Parallel cable, PC		
15	PC		
16	Shovel		
17	Level		
18	Electrician's Tape		
19	Coloured Tape		
20	Ranger Compass		
21	Brunton Compass		
22	Brunton Mount		
23	Brunton Tripod		
24	Cable Reel & Cable		
25	Measuring Tape		
26	Wire stripper/cutter		
27	Water		
28	Salt		
29	Bentonite or granular clay		
30	Layout Binder & Sheets		
31	Pencils		
32	Map		
33	Analog Ohmmeter		
34	Digital Voltmeter		
35	GPS Receiver		

2.2 Data Acquisition: MSU Phoenix System

2.2.1 Phoenix V5 System

The Phoenix V5 System 2000 is the one of world's leading electromagnetic system for geophysical applications. Phoenix V5 System is applicable in Magnetotelluric (MT) technique, Audio Magnetotelluric (AMT) and Induced Polarization (IP) techniques. The low power, 24-bit acquisition units are small, lightweight, simple to operate, and highly flexible are features of Phoenix system. The instruments are normally configured to use removable CompactFlash cards as the data storage medium (MTU User Guide 1.6, 2005).

Best results are achieved when a remote or far remote site is available for noise-reduction techniques. However, in most surveys, a single, electrically quiet site is chosen, and

a MTU/MTU-A with five channels is installed and left in place as the reference for the duration of the survey.

2.2.2 Data Recording

2.2.2.1 Calibration

Before each survey begins, all the MTU/MTU-As and sensors must be calibrated. Once the equipment is set up, the process takes about 10 minutes for an MTU/MTU-A and one hour or more for sensors. Each calibration must be completed in a single session; it cannot be interrupted and resumed.

In Box calibration, MTU measure own amplitude and phase response for self-generated test signal and record to a file called *.CLB, where * is the box serial number (For example, 1853.CLB for). In Coil calibration, MTU send a calibration signal to the magnetic sensors, measures amplitude and phase response of sensors, and save their results in a file called *.CLC, where * is the coil serial number. There will be three separate file for each magnetic sensor (for example COIL2181.CLC, COIL2406.CLC, COIL2407.CLC).

2.2.2.2 Acquisition Parameter setting

WinHost and WinTabEd programs are used to setting acquisition parameter. WinHost controls an MTU in real time via a cable connection to the PC, whereas WinTabEd saves the control settings in a file, STARTUP.TBL, for later transfer to the CompactFlash card of an MTU. This file controls the operation of the MTU the next time it is powered on. Acquisition parameter setting for a station recorded on 14th Oct 2011 was given below as example.

Open WinTabEd, which main window is shown in figure (2.4). There are many options in window which chosen as for this particular station:

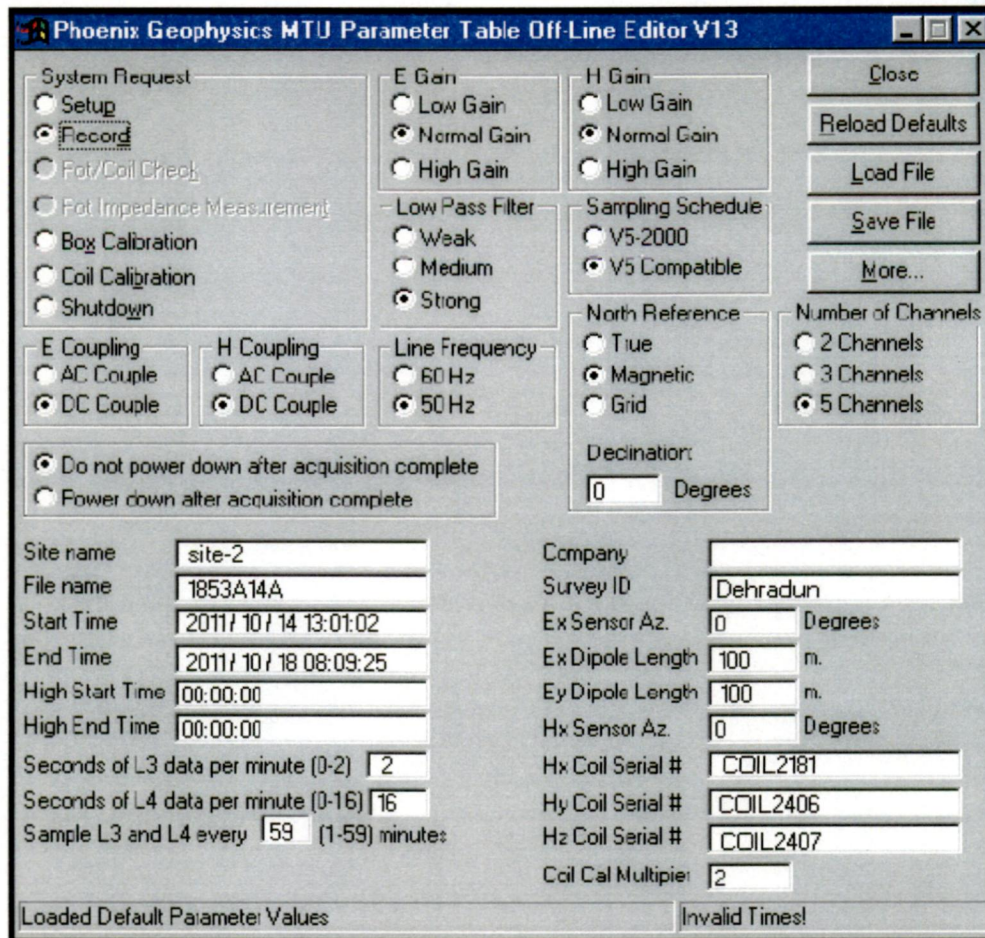


Figure 2.4: WinTabEd main Window

System Request: It should be on “Record” mode, because next time when system MTU system will be on it should record data. Box Calibration and Coil Calibration is used for calibration.

Gain Parameter: E Gain and H Gain settings have three options; Low Gain option is selected for noisy areas, High Gain is chosen when noise level is very low. In most cases Normal Gain gives good results, which is chosen for this site.

Filter parameter: For low contact resistance (<1 kOhm) area select Strong, in high contact resistance (> 10 kOhm) select Weak and in between prefer Medium. In this case contact resistance is 0.1 kOhm so Strong is chosen.

Coupling Parameter: If DC potential is less than 20 mv then DC coupling option gives good data.

Line frequency: 50 Hz is selected, based on frequency of power line.

North Reference and Declination: If your site is oriented in true north direction then True, if it is in magnetic north then Magnetic, otherwise Grid. In case of Magnetic, declination should be

set for survey area, otherwise it would be zero. For this station, in spite of Magnetic north orientation, declination is set to zero, so during processing, it should change.

Acquisition Time parameter: Start time and End time is set as 2011-10-14 13:01:02 and 2011-10-18 08:09:25 respectively. It is a time between which data will be record.

Dipole length: It set as distance between E_x and E_y dipoles, here it is 100 m.

Coil Serial No.: It set as a serial number which printed on magnetic sensor (for example: COIL2181, COIL2406, COIL2407).

Sensor azimuth: Azimuth of sensors and electric dipoles from magnetic north (For this site it set as a zero).

No of channel: Number of MT component which is recording (This site record 5 component).

Site name, File name, Survey ID, Company: Filename fill as format of ssssHdda, where 'sss' represent serial no. of instrument box, 'H' indicate month (in Hexadecimal number system) of data acquisition, 'dd' represent data of acquisition, 'a' represents an alpha character denoting the order of repeated soundings at a single site. Site name, Survey ID, Company fill as you want but maximum 12 characters. 14th Oct site name as 'site-2' and Survey ID is filled 'Dehradun'. File name for this is 1853A14A.

Phoenix system record magnetotelluric data in 3 bands, and save data in three separate file having different extension name (TS3, TS4, and TS5). These files are called **Time series data file**. Primary name of each file is same as define above. Sampling frequency of TS3, TS4 and TS5 file are 2400 Hz, 150 Hz and 15 Hz respectively. TS5 data are sampled continuously, but TS4 and TS3 sampled only periodically. TS3, TS4 and TS5 are also represented by L3, L4, and L5 respectively. Option 'Sample L3 and L4 every (...) minute' set the time slot for periodic sampling. Options 'Seconds of L3 data per minute' and 'Seconds of L4 data per minute' set the number of records (for band L3 it is up to 2 and for band L4 it is up to 16) that can captured at beginning of slot.

After setting of calibration and acquisition parameter, power on the system. There is a LED between N and S. Figure (2.5) shows LED pattern. If everything is proper then it follows normal pattern otherwise alternate patterns shown in figure (2.5). In this figure black colour represent LED flash and white strip show that now LED is not flashing. In normal pattern there are four parts:

- **Instrument status sequence (first seven seconds):** If instrument is performing normally, LED is off for 1 second, then lights continuously for 5 seconds and then goes off for one second. If anything wrong then it blinks rapidly for 350ms as a warning and then flashes from 1 to 7 times. Number of flashes represents warning for which see MTU User Guide 1.6 manual.

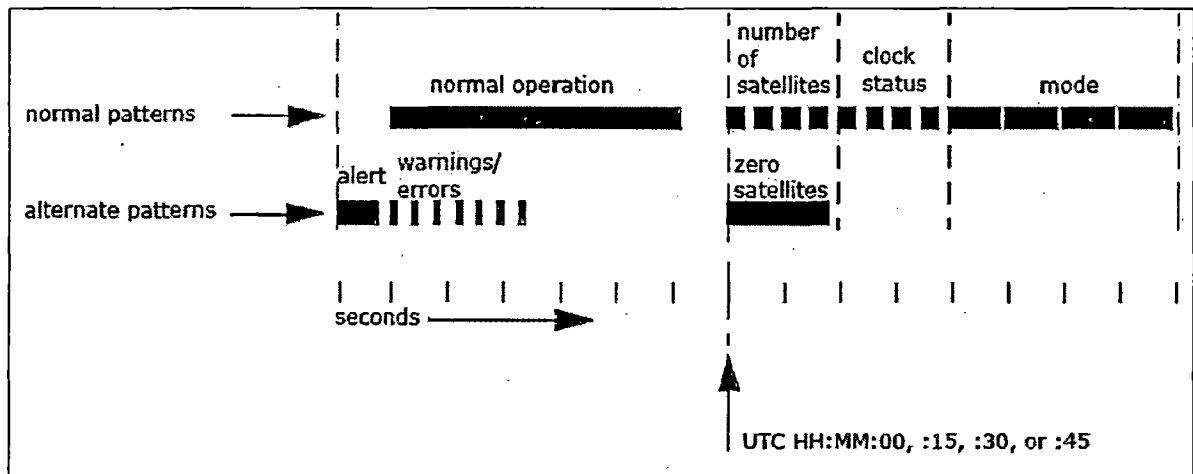


Figure 2.5: LED Pattern for Phoenix data acquisition
(V5 System 2000 MTU/MTU-A User Guide, Version 1.6, September 2005)

- **Satellite lock sequence (next two seconds):** After instrument status sequence, LED pattern is 250ms on, 250ms off for next two second. This represents signal receive from 4 GPS satellite.
- **Clock status sequence (next two seconds):** After receiving signal from satellites, on-board clock synchronizes to GPS time. Clock status sequence is 250ms on, 250ms off, from 0 to four times.
- **Instrument mode sequence (next four seconds):** In these 4 seconds, LED on for 900ms then off for 100ms from 1 to 4 times, depend on instrument mode (setup, standby, recording, or idling after recording).

After completion of data recording, data transferred from CompactFlash card to PC for further processing. Phoenix system saves parameter related to time series and acquisition like Site name, Site co-ordinate, Elevation, Starting and ending time, channel code, etc. in file *.TBL, which is called **Site parameter file**. Data is saved in Time series data file *.TS3, *.TS4 and *.TS5. Time series data are saved in order of the time of the first sample in the record. We recorded data at following 7 stations:

Table 2.2: Phoenix Station Details

S. No.	Station Name and corresponding TBL file	Site Code	Latitude	Longitude	Starting		Ending		Elevation (m)
					Date (dd/mm/yyyy)	Time (hh/mm/ss)	Date (dd/mm/yyyy)	Time (hh/mm/ss)	
1	points-2 (1853A14A)	P2	30:10.423 N	78:05.390 E	14/10/2011	13:01:02	18/10/2011	08:09:25	448
2	base-3 (1852A17A)	B3	30:11.323 N	77:50.176 E	17/10/2011	05:54:02	18/10/2011	04:59:55	389
3	base-3 (1852A18B)	B3	30:11.324 N	77:50.179 E	18/10/2011	06:07:02	24/10/2011	09:00:28	390
4	points-3 (1855A18A)	P3	30:13.424 N	78:12.253 E	18/10/2011	12:36:02	22/10/2011	02:47:52	664
5	points-4 (1853A19A)	P4	30:19.791 N	78:21.483 E	19/10/2011	13:08:02	23/10/2011	08:08:45	1072
6	point-5 (1909A21A)	P5	30:26.946 N	78: 25.594 E	21/10/2011	03:54:02	24/10/2011	08:47:31	819
7	Point-1r (1855A22A)	Pr1	29:49.011 N	77:49.837 E	22/10/2011	11:28:02	23/10/2011	15: 19:23	240

Figure (2.6) shows time span of all Phoenix field data recorded. There are boxes in front of name of each TBL file, which contain:

- a) Time range, written in numbers. It shows starting and ending time of particular TBL file.

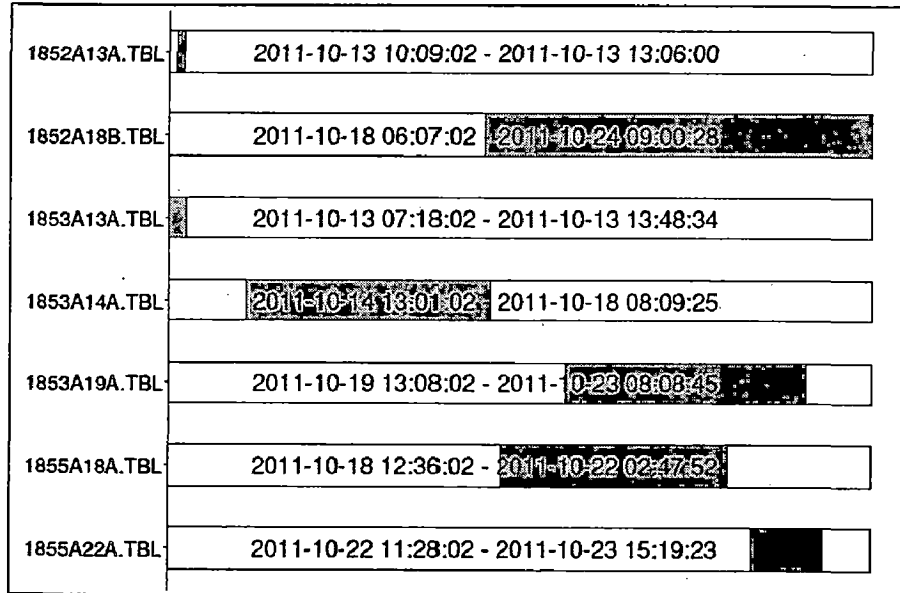


Figure 2.6: Time span of Phoenix Data

- b) Length of box corresponds to time span from smallest starting time to largest ending time among all TBL file.
- c) Length of blue colour show time span of that particular TBL file in respect of total time span.

CHAPTER 3

DATA PROCESSING

Data processing is one of the important steps in any geophysical method. Field data have always various kinds of noises. So data processing directly affect quality of our required result. In case of magnetotelluric method, data processing is very laborious work. Since there are two types of field data recorded: one set of data were recorded by using Metronics System and other set of data were recorded by MSU Phoenix system. First set of data which I used are already processed using MAPROS.

Now my aim is to process recently recorded Phoenix data. First, Phoenix data is processed by software SSMT 2000, but unavailability of original software force to use another software PRC-MTMV developed by GEMRI (Goelectromagnetic Research Institute), Russian academy of Sciences. I take help from Dr. Elena Sokolova, scientist in Goelectromagnetic Research Institute. Processing steps of both software SSMT 2000 and PRC-MTMV is described in following section. Theory and algorithm used in PRC-MTMV code is also described in briefly in further sections.

3.1 Theory of PRC-MTMV

PRC-MTMV code uses multilevel robust averaging method for processing of Magnetotelluric data. We mainly focus on component of EM field transfer operators. More accurate synchronization using new observation systems, leads to good estimation of single-site transfer operators (impedance Z and tipper W_z) and the estimation of other geomagnetic transfer operators like, the horizontal magnetic tensor M and the simultaneous tipper S_z . Definition of transfer operators were discussed in chapter (1.3.1). The system of transfer operators $\{Z, W_z, M, \text{ and } S_z\}$ is sufficient for any interpretation.

During processing of simultaneous EM time series, we will face following problems:

- estimation of the system of transfer operators $\{Z, W_z, M, S_z\}$;
- stabilizing the inferred estimates against time and suppression of noise;
- Noise suppression arising from the combined processing of simultaneous EM observations at several sites; and
- Control of accuracy of transfer operator estimation

Basic principle of theory is to analysis of EM time series and estimation of impedance tensor in the frequency domain. In this theory, problem of processing is solved in following steps: In first step we divide the whole time series into many windows (segments) of different time span and then convert the initial equidistant frequency scale to logarithmically equidistant frequency scale and then it involve determination of mean square of estimates of transfer operators for individual segments of records. After first step, problem of selection and weighting of the data can be solved. Then finally take robust averaging of all partial estimates (Varentsov et al., 2002). These steps are elaborated in next section with taking transfer operator Z as an example.

- Pre-processing of initial time series;
- Spectral analysis of an each record segment (number i);
- Estimation of transfer operators by minimization of least square problem;
- According to Local and Global coherency criteria, selection of partial estimates for a given segment; and
- Multilevel robust averaging of selected partial estimates.

3.1.1 Pre-processing and Spectral Analysis

Pre-processing includes steps before handling EM data in the frequency domain In many cases, the initial pre-processing (selection and decimation of data) of EM time series was done during the recording of digital EM signals. And then some instrument-related pre-processing performed which take care of specific encoding properties of data, that is conversion of time series from specific encoded form to standard form, so it can handle easily. After conversion of data to standard form, target is to removal of outlier and record gaps, additional filtering, and removal of low-frequency trends. These steps should be performed very carefully that maintain the quality of data and not introduce any distortions because that will be very difficult to remove in further processing stages (Ernst et al., 2001).

The selection of length of window for the Fourier transformation is determined by the following two factors: First factor is spectral resolution which depends on length window, and second is the need for a sufficient number of windows $\{W_m, m=1, 2 \dots, M\}$ of various length L_m in the further stacking estimations. These two factors are opposite in sense, and thus we usually carefully observe the data records several times independently with a number of windows of different lengths to get a proper balance of resolution and stability. Spectral

analysis i.e. Fourier transform of time series using FFT scheme requires that the window width be specified as $L_m = 2^n$. Usually, the largest window length is set to be about 3-4 times the longest period estimated and can be as large as 2^{16} samples. Further, window length is obtained as a rule by subdivision of the previous one: $L_{m-1} = L_m/a_m$ with a_m selected as 2 or 4. Windows overlapping is usually ranging within 0-60%, in some cases it goes to 80%. The total number of windows is from first tens to hundreds and first thousands, depending on the total amount and quality of the processed material (Ernst et al., 2001).

The final step of spectral completed with calculation of discrete Fourier transform by FFT algorithm. The spectra obtained are subjected to defiltering to take into account the known frequency responses of the measuring channels.

3.1.2 Transfer Functions Estimation for single Segment

In this section we are focus to calculate the impedance estimate for particular spectral window length. The linear impedance tensor Z connects frequency domain horizontal electric and magnetic field vectors S_E and S_H (Cagniard, 1953):

$$S_E(\omega) = Z(\omega) S_H(\omega) \quad (3.1)$$

These impedance estimates are presented at the log frequency axis. So impedance estimate at each fixed frequency of a logarithmically equidistant grid $\Omega^{TF} = \{\omega_l, l = 1, 2, \dots, L\}$ can be determined from the solution of the following misfit minimization problem:

$$\|S_E(\omega_k) - Z_l S_H(\omega_k)\|^2 = \min, \quad \omega_k \in V_l^{p_0} \quad (3.2)$$

Here we assume that Z_l is constant in range $V_l^{p_0} = [\omega_{l-p_0}, \omega_{l+p_0}]$, $p_0 > 0$. The number of frequencies ω_k in this range constraint the smoothing of low frequency estimates.

This least square problem is solved locally on the i^{th} window of length L_m :

$${}^{(i,m)}Z_l = Z_l = (S_{HH})^{-1} S_{HE} \quad (3.3)$$

Where elements of matrices S_{HE} and S_{HH} are least square averaged cross and auto spectra calculated from original estimates, belonging to the $V_l^{p_0}$. Cross spectra of two signals is a measure of correlation between them. It is defined as:

$$S_{HE} = H \cdot E^*$$

Where E^* represent conjugate of signal E. If both signal are same then it refer as auto spectra. Parameter p_0 depend on the number of frequencies in the estimation frequency grid Ω^{TF} and generally it is unity but if frequency grid is large then it may be increased.

This solution does not depend on electric field auto-spectra, which is generally more affected by noise, and is naturally extended for the remote reference (RR) sounding scheme with additional magnetic field observation R in the remote site:

$${}^{(i,m)}Z_l^{RR} = Z_l^{RR} = (S_{RH})^{-1}S_{RE} \quad (3.4)$$

Where matrices S_{RH} and S_{RE} contain only cross spectra of respective field components with remote site in the neighborhood $V_l^{p_0}$ (Varentsov et al., 2002).

The quality of the solutions obtained from equation (3.3) is depending on the misfit in relation (3.2) and can be expressed in the form of confidence intervals and different coherency estimates (mutual and partial). We will use impedance confidence intervals δZ_l , which is common for impedance amplitude and both real and imaginary parts, and squared coherency estimates multiple $co2_{EH} = coh_{EH}^2 = \{ coh_{E_jH}^2(\omega_l), j = x, y; \omega \in \Omega^{TF} \}$ and partial $co2_{HH} = coh_{HH}^2 = \{ coh_{H_lH}^2(\omega_l), l \in \Omega^{TF} \}$ (Gamble et al., 1979b; Semenov, 1985). Both these local coherency estimates on the Ω^{TF} grid and their mean-square norm on this grid will be taken account.

3.1.3 Averaging of Transfer Operators over set of partial estimates

In this section we averaged partial estimates of the impedance over a set of record segments has a fixed length L_m . We build a procedure ${}^{(i,m)}Z_l$ for weighted i to averaging the set $\{ {}^{(i,m)}Z_l \}$. In this method, we select only those data that satisfy Global and local coherency criteria. A global coherency criterion is one which should satisfy by all data of individual segments and local criteria should satisfy by values of the impedance components at individual frequencies. In *bicoordinate* scheme (equation 3.4), estimates are averaged over segment index i and simultaneously we average them over frequency range $V_l^{p_1} = [\omega_{l-p_1}, \omega_{l+p_1}]$, $p_1 > 0$. Since statistical moments of partial estimates are successively accumulated for each globally selected window so this procedure is cumulative (Varentsov et al., 2002). Averaged Impedance is divided by the function $\omega^{1/2}$ to terminate the predominant frequency dependence. Impedance ${}^{(m)}Z_l$ and its confidence interval ${}^{(m)}\delta Z_l$ can be written as:

$${}^{(m)}Z_l = S_{WZ} / S_W \quad (3.5.1)$$

$${}^{(m)}\delta Z_l = \max \left\{ \frac{1}{S_W}, \theta \sqrt{\frac{S_{WZ^2} / S_W - ({}^{(m)}Z_l^2)}{N_s}} \right\} \quad (3.5.2)$$

$$S_W = \sum ({}^{(i_s)}w_{l_s}), \quad S_{WZ} = \sum ({}^{(i_s)}w_{l_s}) Z_{l_s}$$

$$S_{WZ^2} = \sum ({}^{(i_s)}w_{l_s}) Z_{l_s}^2, \quad \Sigma = \sum_{i_s, l_s}$$

Where i_s is the index of a globally selected window; l_s is the frequency index of data locally selected inside the V_l^{p1} ; N_s is the final number of the data selected; θ is the Fisher confidence factor from the segment [1,2]; and the index m of partial estimates of the impedance and weights is omitted (Varentsov et al., 2002).

The weights $({}^{(i_s)}w_{l_s})$ are defined from local confidence intervals estimated for the i_s spectral window:

$${}^{(i_s)}w_{l_s} = \frac{1}{({}^{(i_s)}\delta Z_{l_s}^2 + ({}^{(i_s)}\Delta_{l_s}^2)} \quad (3.6)$$

This includes the confidence intervals of initial impedance estimates and the additional elements $({}^{(i_s)}\Delta_{l_s}^2)$.

The criterion for the “global” selection is based on the average coherency estimates $co2_{E_1H}$, $co2_{E_2H}$ and $co2_H$ for the whole segments:

$$co2_{E_jH} \geq \varepsilon_{1j}^G, \quad j = x, y; \quad (3.7.1)$$

$$co2_H \leq \varepsilon_2^G \quad (3.7.2)$$

analysis i.e. Fourier transform of time series using FFT scheme requires that the window width be specified as $L_m = 2^n$. Usually, the largest window length is set to be about 3-4 times the longest period estimated and can be as large as 2^{16} samples. Further, window length is obtained as a rule by subdivision of the previous one: $L_{m-1} = L_m/a_m$ with a_m selected as 2 or 4. Windows overlapping is usually ranging within 0-60%, in some cases it goes to 80%. The total number of windows is from first tens to hundreds and first thousands, depending on the total amount and quality of the processed material (Ernst et al., 2001).

The final step of spectral completed with calculation of discrete Fourier transform by FFT algorithm. The spectra obtained are subjected to defiltering to take into account the known frequency responses of the measuring channels.

3.1.2 Transfer Functions Estimation for single Segment

In this section we are focus to calculate the impedance estimate for particular spectral window length. The linear impedance tensor Z connects frequency domain horizontal electric and magnetic field vectors S_E and S_H (Cagniard, 1953):

$$S_E(\omega) = Z(\omega) S_H(\omega) \quad (3.1)$$

These impedance estimates are presented at the log frequency axis. So impedance estimate at each fixed frequency of a logarithmically equidistant grid $\Omega^{TF} = \{\omega_l, l = 1, 2, \dots, L\}$ can be determined from the solution of the following misfit minimization problem:

$$\|S_E(\omega_k) - Z_l S_H(\omega_k)\|^2 = \min, \quad \omega_k \in V_l^{p_0} \quad (3.2)$$

Here we assume that Z_l is constant in range $V_l^{p_0} = [\omega_{l-p_0}, \omega_{l+p_0}]$, $p_0 > 0$. The number of frequencies ω_k in this range constraint the smoothing of low frequency estimates.

This least square problem is solved locally on the i^{th} window of length L_m :

$${}^{(i,m)}Z_l = Z_l = (S_{HH})^{-1} S_{HE} \quad (3.3)$$

Where elements of matrices S_{HE} and S_{HH} are least square averaged cross and auto spectra calculated from original estimates, belonging to the $V_l^{p_0}$. Cross spectra of two signals is a measure of correlation between them. It is defined as:

$$S_{HE} = H \cdot E^*$$

Where E^* represent conjugate of signal E. If both signal are same then it refer as auto spectra. Parameter p_0 depend on the number of frequencies in the estimation frequency grid Ω^{TF} and generally it is unity but if frequency grid is large then it may be increased.

This solution does not depend on electric field auto-spectra, which is generally more affected by noise, and is naturally extended for the remote reference (RR) sounding scheme with additional magnetic field observation R in the remote site:

$${}^{(i,m)}Z_l^{RR} = Z_l^{RR} = (S_{RH})^{-1}S_{RE} \quad (3.4)$$

Where matrices S_{RH} and S_{RE} contain only cross spectra of respective field components with remote site in the neighborhood $V_l^{p_0}$ (Varentsov et al., 2002).

The quality of the solutions obtained from equation (3.3) is depending on the misfit in relation (3.2) and can be expressed in the form of confidence intervals and different coherency estimates (mutual and partial). We will use impedance confidence intervals δZ_l , which is common for impedance amplitude and both real and imaginary parts, and squared coherency estimates multiple $co2_{EH} = coh_{EH}^2 = \{coh_{E,H}^2(\omega_l), j = x, y; \omega \in \Omega^{TF}\}$ and partial $co2_{HH} = coh_{HH}^2 = \{coh_{H,H}^2(\omega_l), l \in \Omega^{TF}\}$ (Gamble et al., 1979b; Semenov, 1985). Both these local coherency estimates on the Ω^{TF} grid and their mean-square norm on this grid will be taken account.

3.1.3 Averaging of Transfer Operators over set of partial estimates

In this section we averaged partial estimates of the impedance over a set of record segments has a fixed length L_m . We build a procedure ${}^{(i,m)}Z_l$ for weighted i to averaging the set $\{{}^{(i,m)}Z_l\}$. In this method, we select only those data that satisfy Global and local coherency criteria. A global coherency criterion is one which should satisfy by all data of individual segments and local criteria should satisfy by values of the impedance components at individual frequencies. In *bicoordinate* scheme (equation 3.4), estimates are averaged over segment index i and simultaneously we average them over frequency range $V_l^{p_1} = [\omega_{l-p_1}, \omega_{l+p_1}]$, $p_1 > 0$. Since statistical moments of partial estimates are successively accumulated for each globally selected window so this procedure is cumulative (Varentsov et al., 2002). Averaged Impedance is divided by the function $\omega^{1/2}$ to terminate the predominant frequency dependence. Impedance ${}^{(m)}Z_l$ and its confidence interval ${}^{(m)}\delta Z_l$ can be written as:

$${}^{(m)}Z_l = S_{WZ} / S_W \quad (3.5.1)$$

$${}^{(m)}\delta Z_l = \max \left\{ \frac{1}{S_W}, \theta \sqrt{\frac{S_{WZ^2} / S_W - ({}^{(m)}Z_l)^2}{N_s}} \right\} \quad (3.5.2)$$

$$S_W = \sum ({}^{(i_s)}W_{l_s}), \quad S_{WZ} = \sum ({}^{(i_s)}W_{l_s} ({}^{(i_s)}Z_{l_s}))$$

$$S_{WZ^2} = \sum ({}^{(i_s)}W_{l_s} ({}^{(i_s)}Z_{l_s}^2)), \quad \Sigma = \sum_{i_s, l_s}$$

Where i_s is the index of a globally selected window; l_s is the frequency index of data locally selected inside the V_l^{p1} ; N_s is the final number of the data selected; θ is the Fisher confidence factor from the segment [1,2]; and the index m of partial estimates of the impedance and weights is omitted (Varentsov et al., 2002).

The weights $({}^{(i_s)}W_{l_s})$ are defined from local confidence intervals estimated for the i_s spectral window:

$${}^{(i_s)}W_{l_s} = \frac{1}{({}^{(i_s)}\delta Z_{l_s}^2 + ({}^{(i_s)}\Delta_{l_s}^2)} \quad (3.6)$$

This includes the confidence intervals of initial impedance estimates and the additional elements $({}^{(i_s)}\Delta_{l_s}^2)$.

The criterion for the “global” selection is based on the average coherency estimates $CO2_{E_1H}$, $CO2_{E_2H}$ and $CO2_H$ for the whole segments:

$$CO2_{E_jH} \geq \varepsilon_{1j}^G, \quad j = x, y; \quad (3.7.1)$$

$$CO2_H \leq \varepsilon_2^G \quad (3.7.2)$$

All data for current window are rejected if any of these conditions violated. Common range for $\varepsilon_{1j}^G = 0.6 - 0.8$ and $\varepsilon_2^G = 0.7 - 0.9$. These values depend upon the amount and quality of data processed and the error distribution within the frequency range considered.

Local selection criteria of ${}^{(i,m)}Z_l$ among the segments which satisfy global selection criterion (3.6), given by these two relation:

$$CO2_{EjH} = \varepsilon_{1j}^L, \quad j = x, y \quad (3.8.1)$$

$$CO2_H = \varepsilon_2^L \quad (3.8.2)$$

These new constants ε_{1j}^L and ε_2^L have value close to the global constants ε_{1j}^G and ε_2^G .

Selected impedance values are further averaged according to relation (3.4) at each frequency within V_l^{P1} . Quality of data can be improved if number N_s of partial estimates which satisfy both local and global selection criterion is calculated accurately. Data selection criterion controls the stability of first-level averaging (Varentsov et al., 2002).

3.1.4 Averaging over multi-window

Now our next step is second-level robust averaging. Multiwindow averaging is beneficial in diminishing non stationary effects which depend on windows width. The averaging is done by bicoordinate scheme (Equation 3.5) which already described, but this time we use this without selection criteria. There is smallest modification in frequency grid V_l^{P2} . With this averaging method we determine weighting factor which help to suppress the outlier (Varentsov et al., 2002).

3.1.5 Multi-RR Estimation

A robust procedure of multi-RR estimation with the frequency averaging parameter p_3 is constructed (similar to the above multiwindow averaging) for the sequence of final RR estimates $\{{}^{(n)}Z^{RR}, n = 1, \dots, N^{RR}\}$ in a series of N^{RR} remote sites (Varentsov et al., 2002).

3.1.6 Estimating Geomagnetic Transfer Functions

In above sections, we described the robust processing scheme for impedance estimation. In this theory, impedance Z is taken as example for description of this scheme. This scheme can apply for estimation of other geomagnetic transfer operators with minor changes (Varentsov et al., 2002).

3.2 Field Data Processing: Phoenix Time series

3.2.1 SSMT 2000 Processing

There are four types of files in Phoenix system: Site parameter file (*.TBL), Time series data file (*.TSn), Instrument Calibration file (.CLB) and Sensor Calibration file (.CLC). SSMT software is used for processing of MT data recorded by Phoenix system. Each steps of processing is described below:

- 1) Start SSMT software, following window appear;

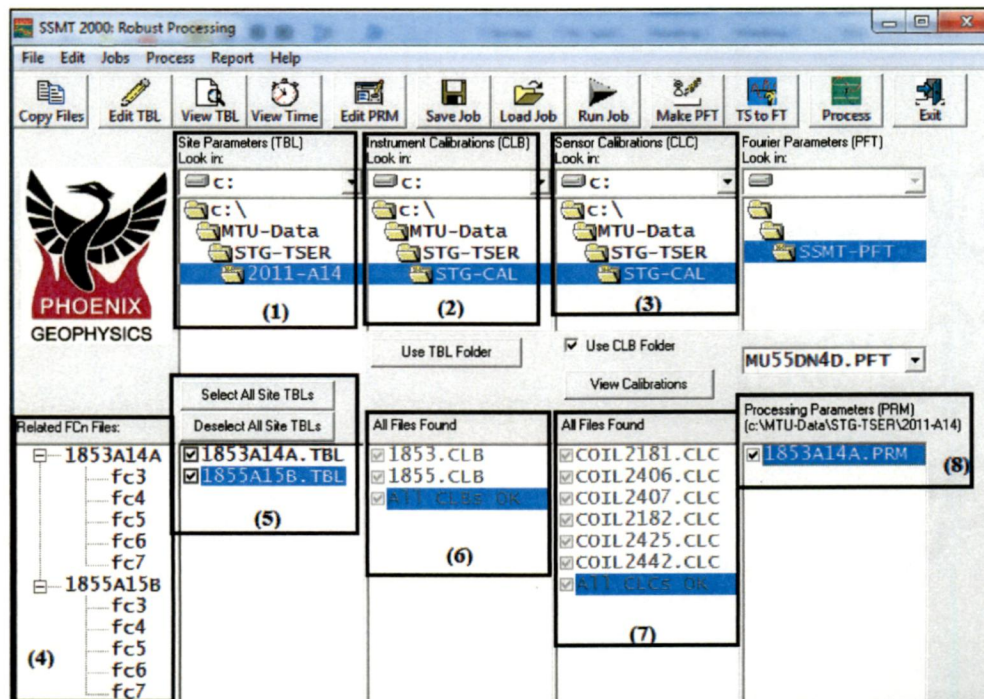


Figure 3.1: Main window of SSMT 2000

This window is divided in 8 sections to understand processing.

Section (1): Browse to folder of site parameter file,

Section (2): Browse to folder of Instrument Calibration file,

Section (3): Browse to folder of Sensor Calibration file,

After locating input files, select appropriate site parameter file from section (5) which have to process. Automatically corresponding instrument calibration file and sensor calibration file will appear in section (6) and (7).

2) 'Edit TBL' option used when any editing required in site parameter file. 'View Time' show time span of all selected TBL file as figure (2.6). This figure shows time span of all Phoenix field data recorded by us.

3) Click on 'Make PFT' option, following window appear:

Band (Level)	Starting Frequency	Frequencies in Top Octave	Number of Octaves	Record Interval	Overlap
2	--	--	--	--	--
3	352.94118	1	4	1	1
4	35	3	3	4	1
5	5	4	4	30	1
6	0.3125	4	5	60	2
7	0.00976562	4	5	600	4
8	--	--	--	--	--

Figure 3.2: Window of setting for PFT file

Here set parameters for producing Fourier transform of time series. Brief description of parameters is as:

- a) **Input Data type:** For normal processing select Measured Field. If data were recorded parallel for testing then select White noise test. If data were recorded for continuous monitoring application then choose hourly files.
- b) **Output Data Format:** This option determines the number of frequency in the output data. For more resolution select '4 frequencies per octave' otherwise '2 frequencies per octave'.
- c) **Bands:** This option determines the number of band will be processed. Different bands for phoenix data were discussed in chapter 2.2.2.2.
- d) **Processing Times:** This is used for limiting the time range for processing.

After setting parameters (default setting is sufficient for normal processing) save Fourier transform parameter file and select 'TS to FT' option for Fourier transform. Software takes some times to calculate spectra and output files (* .Fcn) appears in Section (4) of Figure (3.1) corresponding to each *.TSn file.

4) Now click on 'Edit PRM' option which shows following dialog box:

Figure 3.3: Window of setting for PRM file

- a) **Select Robust Processing Parameters:** Two option Coherency and Rho variance controlled the noisy data and suppress them according to set criteria. It reduces error bars and smooth's the curve. Coherency type refer to 8 type of coherency, which are different combination of Multiple and Partial coherency for electric and magnetic components.
- 1 to combine Type 2 with Type 3.
 - 2 to use the Multiple Coherency of Ex with the total magnetic field.
 - 3 to use the Multiple Coherency of Ey with the total magnetic field.
 - 4 to combine Type 5 with Type 6.
 - 5 to use the Partial Coherency of Ex with the total magnetic field.
 - 6 to use the Partial Coherency of Ey with the total magnetic field.
 - 7 to use the combined factors of the Multiple Coherency of Hx with the total Remote Magnetic field and the Multiple Coherency of Hy with the total Remote Magnetic field.
 - 8 to use the combined factors of the Partial Coherency of Hx with the total Remote Magnetic field and the Partial Coherency of Hy with the total Remote Magnetic field.
- b) **'Maximum fraction of estimates to reject'** option set a value for rejection of that fraction of data if data does not reach to set value in each attempt.
- c) **Maximum Crosspowers:** This is the number of segments in which time series is divided for calculation of estimates for each frequency and then averaged over no of segments.
- d) **Weight Type:** Rho Variance option gives more weight to data having less error bar while Coherency option gives them which have large coherency.
- e) **Weight cut-off value:** If weight assigned to data is less than this value then it reduced to zero otherwise not.

After setting parameter save processing parameter file (Ex. 1853A14A.PRM) and click on option 'Process'. Processing of time series take longer time and after completion generate three types of output file (*.MTH, *.MTR and *.MTL). Each files corresponding to different frequency ranges (MTH- 10^3 - 10^{-1} ; MTL- 10^0 - 10^{-3} ; MTR- 10^{-2} - 10^{-5}). MT-PLOT software used

output files for plotting of different component like apparent resistivity, phase etc. Plot of apparent resistivity and phase using MT-PLOT is shown following figure (3.4):

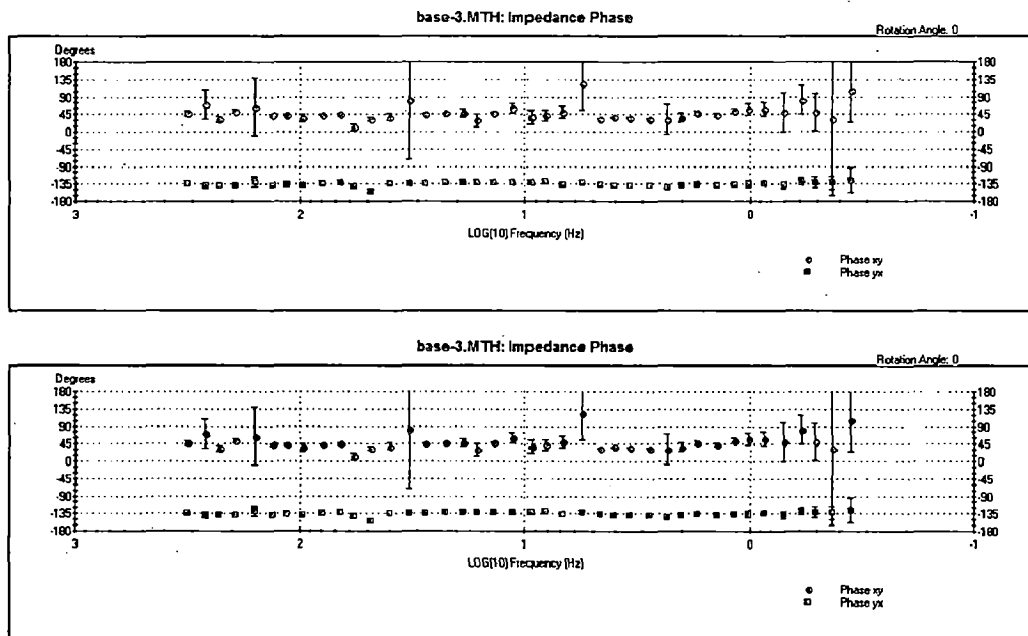


Figure 3.4: Apparent resistivity and phase plot for base-3 station using MT-PLOT

- 5) Further, output files can be edited and converted in EDI file using MTEDITOR software. (Due to demo version of software, I couldn't perform this step, so I used different scheme (PRC-MTMV) for processing.

3.3 PRC-MTMV Processing

In this section, different stages of processing of Phoenix data using PRC-MTMV are illustrated. I processed data of one station point-3, with help of Dr. Elena Sokolova. Each processing step with plots and figures are described below:

- 1) Data recorded by Phoenix system are saved as file of extension name *.TSn and *.TBL. There are also instrument and sensor calibration file *.CLB and *.CLC. These files are specifically encoded. So first convert them into standard form using PRC-MTMV code. 1855A18A.TS5 files converted two file having extension name PRB and PRC. Calibration and 1855A18A.TBL file combined converted into channel

response file having extension name *.CHN which contain information of amplitude and phase response of system for different frequency. Screenshot of *.CHN file is shown in figure (3.5). First column is frequency, other are response (modulus and argument) for each field component.

#	'#FP'	99	5 / NTF,NCH	ORIGINAL CONJUGATED SCALED (MOD,ARG)							
			'#EX'	'#EY'	'#EX'	'#EY'	'#EX'	'#EY'	'#EX'	'#EY'	
1	11585	0.15990	0.06	0.16040	0.06	0.141900E-03	-89.92	0.144400E-03	-89.92	0.14790E-03	-89.92
2	9741.8	0.15990	0.07	0.16040	0.07	0.168800E-03	-89.91	0.171700E-03	-89.91	0.17590E-03	-89.91
3	8192	0.15990	0.08	0.16040	0.08	0.200700E-03	-89.89	0.204200E-03	-89.89	0.20920E-03	-89.89
4	6888.5	0.15990	0.10	0.16040	0.10	0.238700E-03	-89.87	0.242800E-03	-89.87	0.24880E-03	-89.87
5	5792.7	0.15990	0.12	0.16040	0.12	0.283800E-03	-89.84	0.289900E-03	-89.84	0.29590E-03	-89.84
6	4870.9	0.15990	0.14	0.16040	0.14	0.337500E-03	-89.81	0.343400E-03	-89.81	0.35190E-03	-89.81
7	4096	0.15990	0.17	0.16040	0.17	0.401400E-03	-89.78	0.408400E-03	-89.78	0.41840E-03	-89.78
8	3444.4	0.15990	0.20	0.16030	0.20	0.477310E-03	-89.74	0.485610E-03	-89.74	0.49761E-03	-89.73
9	2896.3	0.15990	0.24	0.16030	0.24	0.567610E-03	-89.69	0.577510E-03	-89.69	0.59171E-03	-89.68
10	2435.5	0.15990	0.28	0.16030	0.28	0.675010E-03	-89.63	0.686810E-03	-89.63	0.70372E-03	-89.62
11	2048	0.15990	0.34	0.16030	0.34	0.802720E-03	-89.56	0.816720E-03	-89.56	0.83683E-03	-89.55
12	1722.1	0.15990	0.40	0.16030	0.40	0.954640E-03	-89.47	0.971240E-03	-89.47	0.99514E-03	-89.47
13	1448.2	0.15991	0.48	0.16031	0.48	0.113510E-02	-89.37	0.115510E-02	-89.37	0.11831E-02	-89.37
14	1217.7	0.15991	0.57	0.16031	0.57	0.135010E-02	-89.25	0.137310E-02	-89.25	0.14071E-02	-89.25

Figure 3.5: Screenshot of *.CHN file

File with extension name PRC is a header file which screenshot is shown in figure (3.6), contains information of Start time (2011/10/18; 12:36:02), End time (2011/10/22; 02:47:53), time interval (0.06667), Number of sample (4654605), Field component name (E_x, E_y, H_x, H_y, H_z), scaling factor (-1 for electric and 1 for magnetic) etc.

#	Text
1	* PHOENIX TBL/TS5 TIME SERIES
2	* CONVERTED INTO PRC/PRB FORMAT
3	'#DT' 1 4654605 -4096 0.666666701436E-01 5 /
4	* START/STOP TIME: 2011 10 18 12 36 2 2011 10 22 2 47 53 0.000 0 0.000
5	'#FLD' '#EX' -1.0000 4654605 0.666666701436E-01 3 1 /
6	'#FLD' '#EY' -1.0000 4654605 0.666666701436E-01 3 1138 /
7	'#FLD' '#HX' 1.0000 4654605 0.666666701436E-01 3 2275 /
8	'#FLD' '#HY' 1.0000 4654605 0.666666701436E-01 3 3412 /
9	'#FLD' '#HZ' 1.0000 4654605 0.666666701436E-01 3 4549 /
10	

Figure 3.6: Screenshot of *.PRC file

File with extension name PRB is a Binary file which is corresponding to time series data.

- 2) Beside of this conversion of file, two other file created, one of them contains all information of parameters of processing (*.DAT), and second file (*.HED) contain

header for output processed file. In this header site name, Box name, and any other comment.

- 3) All converted files:*.PRB, *.PRC, *.CHN, *.HED and *.DAT is transferred to the folder containing PRC-MTMV code and run PRC-MTMV code further processing. Following screen shot is appeared.

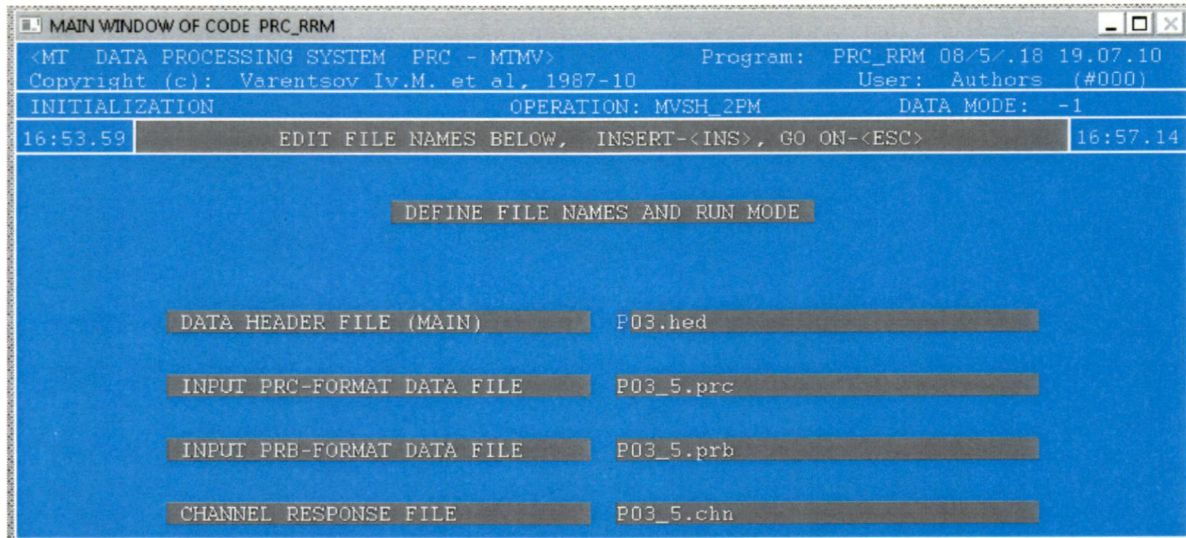


Figure 3.7: Main window of PRC-MTMV

The desired information is supplied in the screen window. Time series can be edited and synchronised if necessary. Many spikes were observed in beginning of E_x and E_y data, so the beginning shifted up to 60 samples to avoid the first severe spike in electric components.

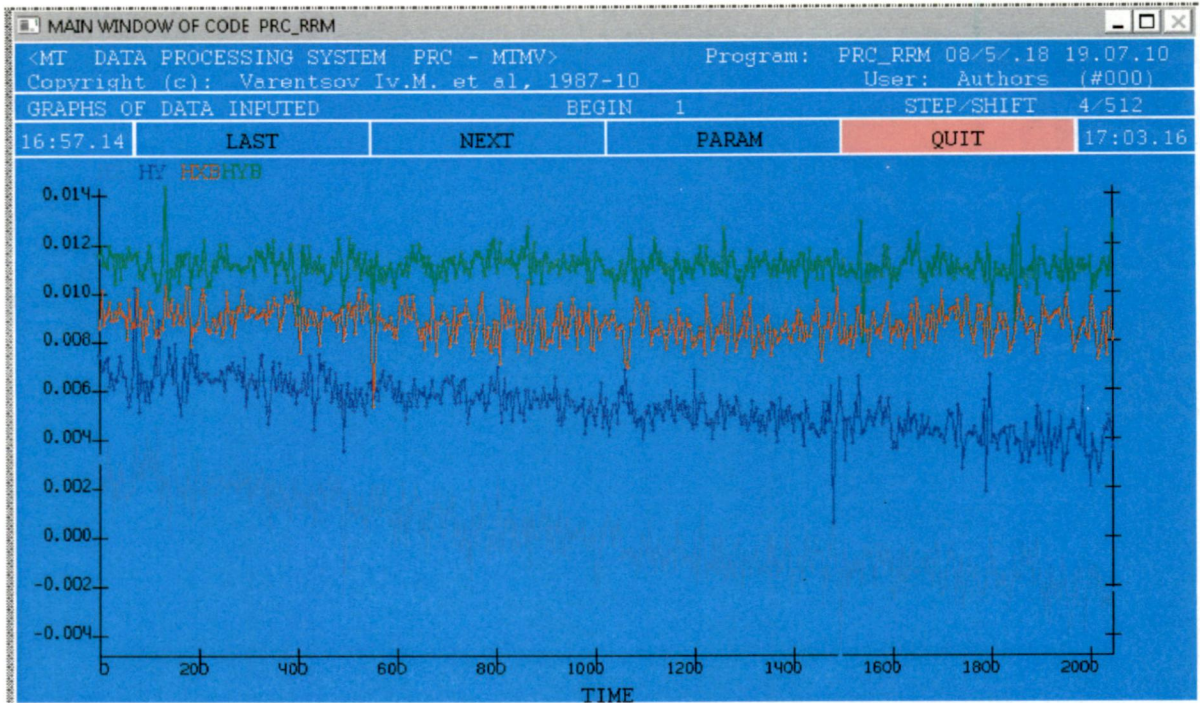


Figure 3.8: Visualisation of time series in PRC-MTMV

4) After editing, run PRC-MTMV code.

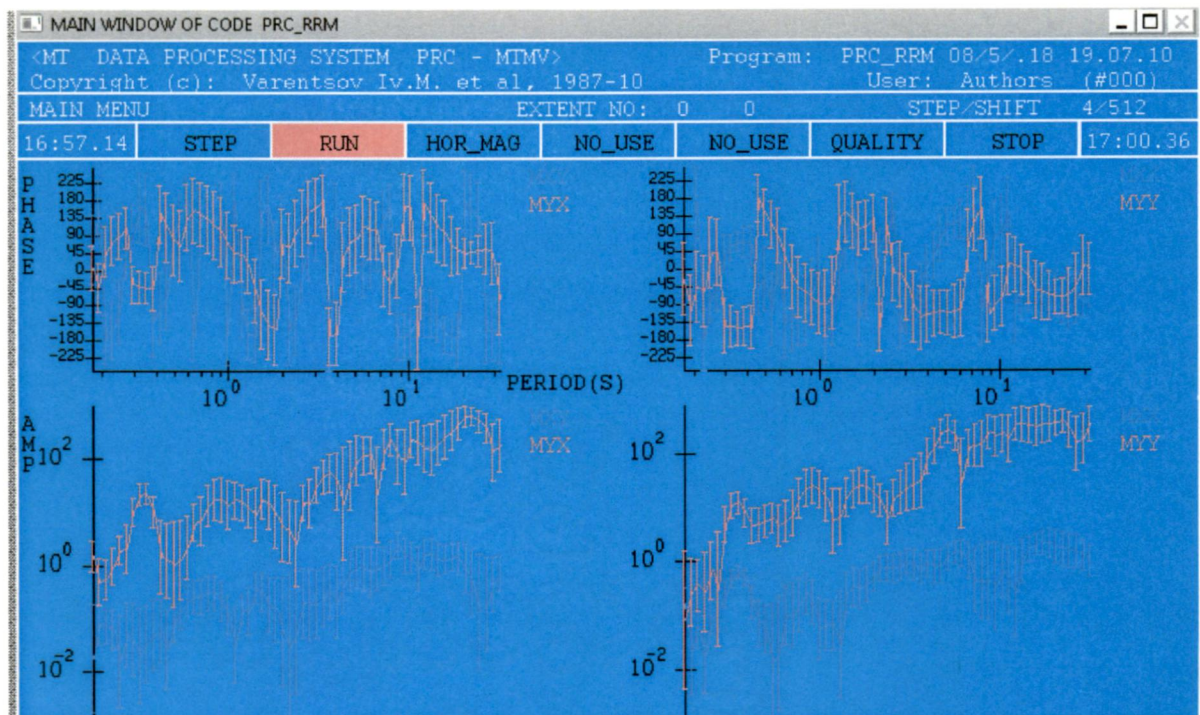


Figure 3.9: Amplitude and Phase plot of transfer operator in PRC-MTMV

During processing it first divide time series into many segments and compute Fourier transform as described in Section 3.1.1. For point-3 station, spectra $\{W_m\}$ divided in $m=10$ windows and their duration, sampling rate, No. of samples, and overlapping is presented in table (3.1).

Table 3.1: Spectral window sequence detail

m	Duration (s)	T_{min}	T_{max}	No. of Time Periods	Width L_m (in samples, $K=1024$)	Overlapping (%)
1	136.533	0.1768	32	61	2K	0
2	273.067	0.1768	64	69	4K	0
3	546.133	0.1768	128	77	8K	0
4	1092.267	0.5	256	73	16K	0
5	2184.533	2	512	65	32K	0
6	4369.067	8	1024	57	64K	40
7	8738.134	32	2435.5	51	128K	50
8	17476.268	64	4096	49	256K	60
9	34952.535	128	8192	49	256K	70
10	69905.070	256	8192	41	256K	80

We have 10 numbers of spectral windows. Then for each record segment it estimate transfer function, misfit in mean square problem from relation (3.2) and different type of coherency (Section 3.1.3). Initially local coherency was set in range of 0.40- 0.50 and global coherency in range of 0.17-0.45 (different for each spectral windows). Further, according to set criteria of coherency partial estimates selected and then averaged on the basis of equation (3.5). For Example, spectral window (1) local coherency is set 0.40 and global coherency 0.45. There are 2272 extent but on basis of coherency criteria, only 1521 were selected. Parameter p_1 , p_2 and p_3 used in averaging were initially set to unit.

5) After completion of processing many types of file generated which are as:

- a) ***.inf file:** This is most important file which contains all coherency (like multiple, partial, input, predictable etc.) value for each segments. It also have detail of quality of data i.e. this much percentage of data have coherency above this value. We carefully observe them and according to Global and Local Selection criteria we make change in processing parameter file and again repeat processing until we don't get satisfactory result. Initially Global coherency
- b) ***.ftf file:** It contains the impedance estimates for each frequency.
- c) There are other intermediate file *.ler, *.lst, and *.rsp file which contain estimates and other intermediate information which calculated during processing. For example *.ler file contain impedance estimate, phase for each extent for all time period. It also content coherency, noise/signal ratio, average of EM field component for all time-period and for all extent. *.ler contain start time (2011/10/18; 12:36:2), end time (2011/10/ 22; 2:47:53).

6) Further, this *.ftf file was used to generate *.EDI file. Using EDI file we can easily plot the estimates. In case of data plot is like cloud take spline approximation. Plot of processed results are shown below:

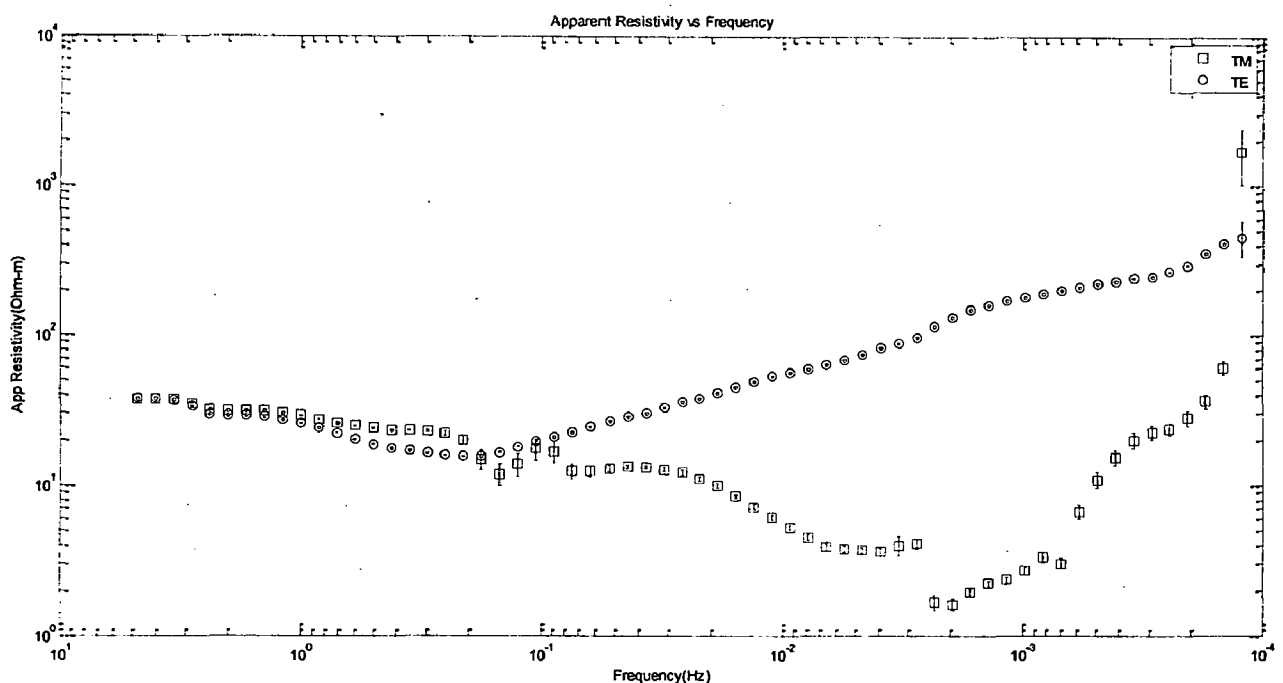


Figure 3.10: Plot of apparent resistivity for point-3 station

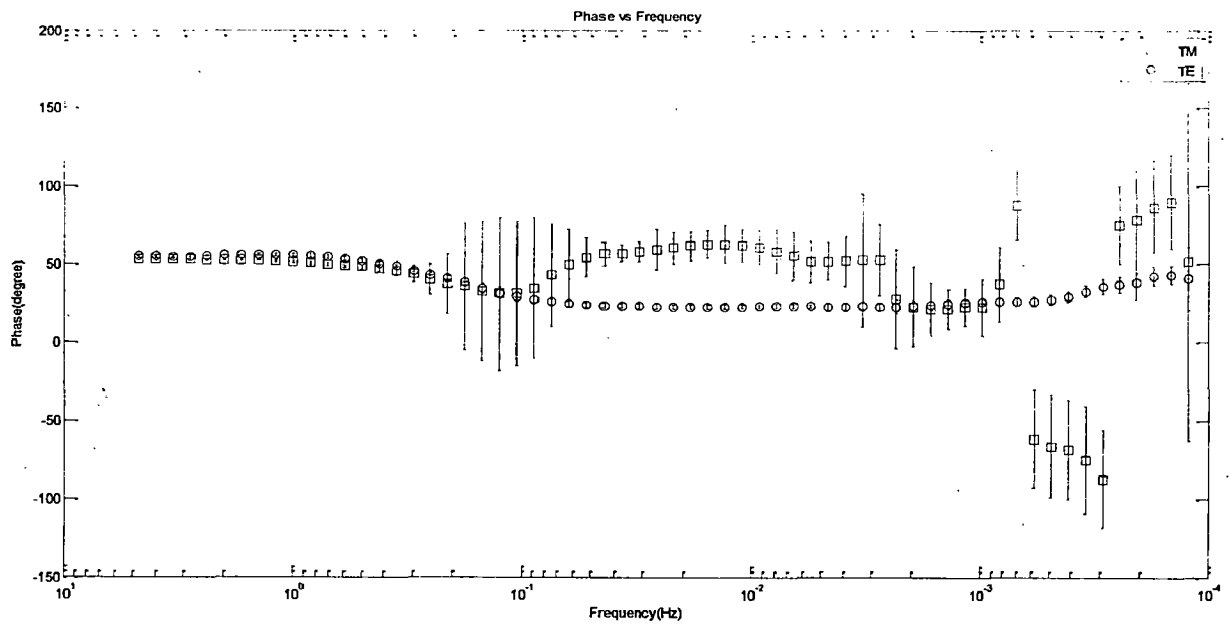
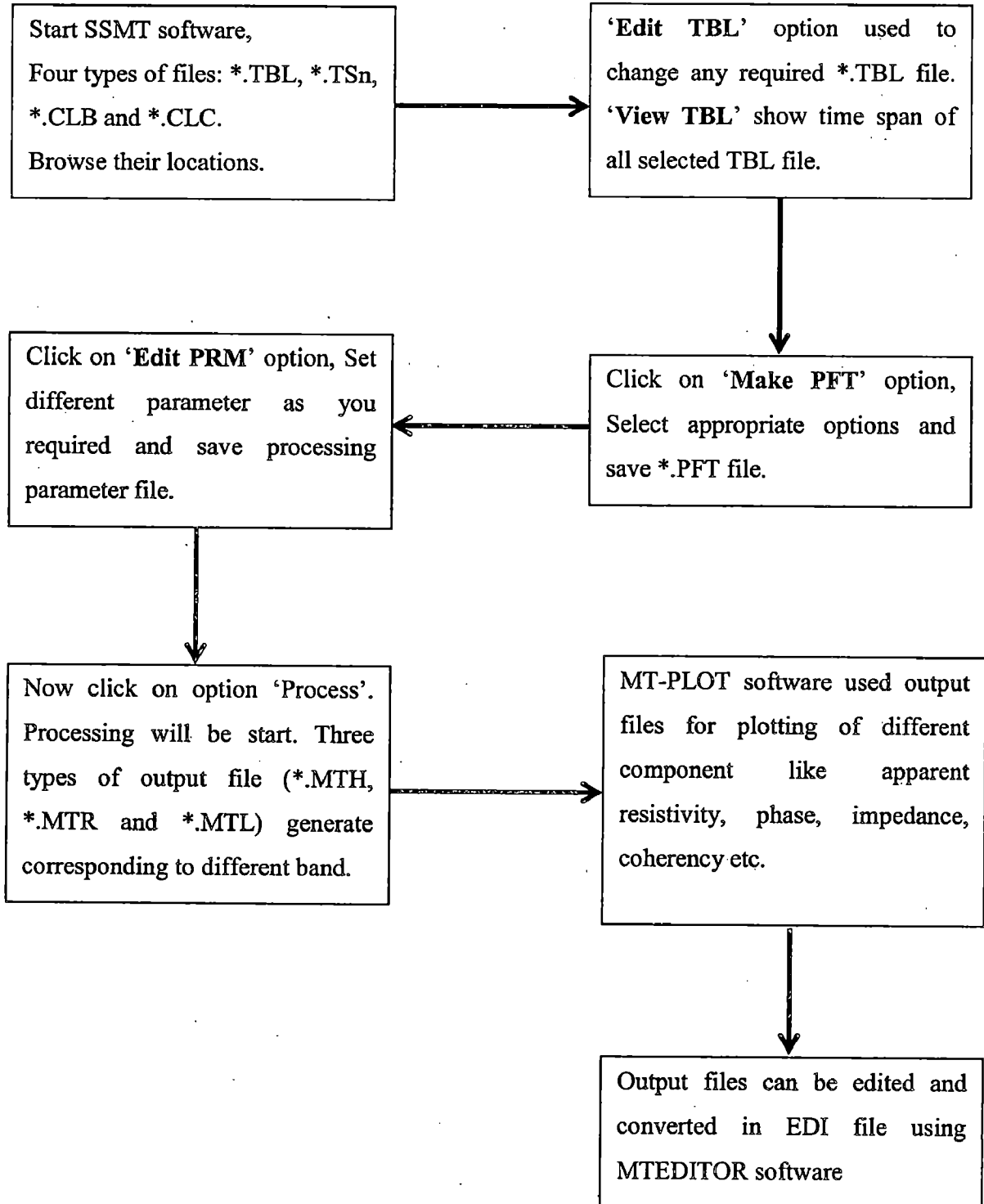


Figure 3.11: Plot of apparent phase for base-3 station

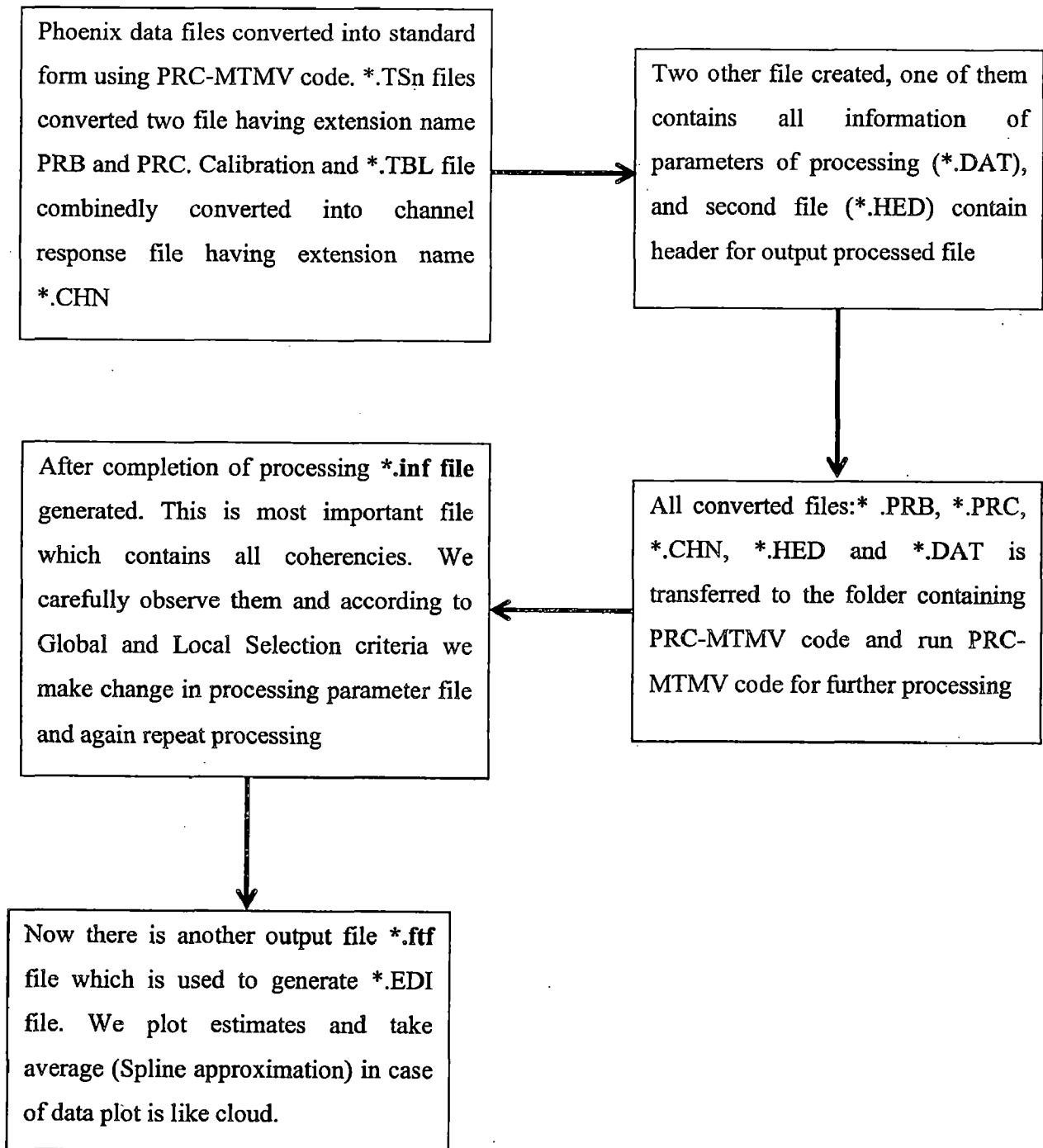
Thus, these are the processing steps for Phoenix data using PRC-MTMV processing code.

3.4 FLOWCHARTS

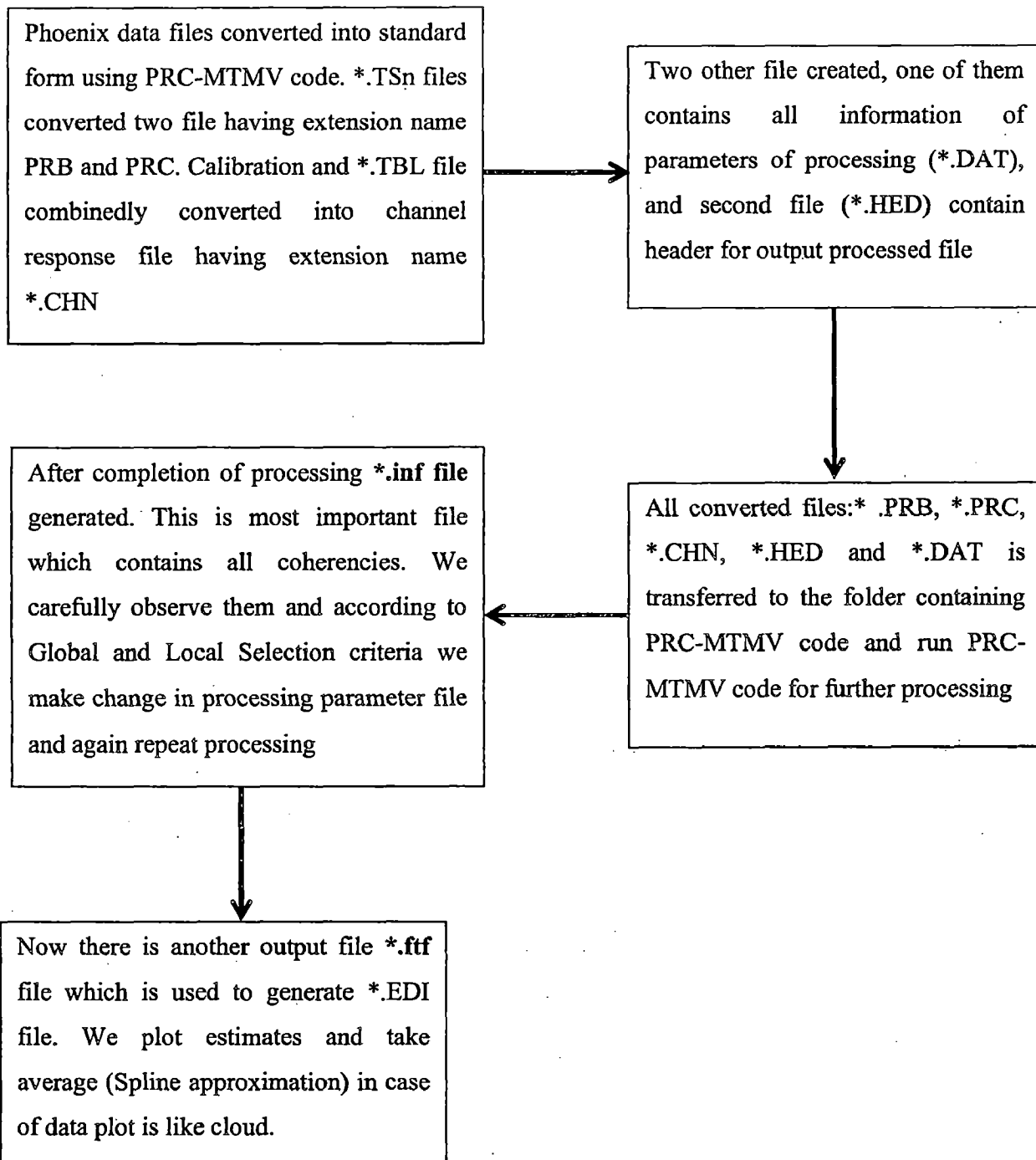
3.4.1 SSMT Processing Flowchart



3.4.2 PRC-MTMV Processing Flowchart



3.4.2 PRC-MTMV Processing Flowchart



CHAPTER 4

2D INVERSION THEORY: MT2DInvMatlab

Inversion is a mathematical method to compute meaningful or compatible result to real using observed data. If model parameter is known then its response computation is called forward modeling. Assuming initial guess model compute its response and reduce error between observed data and computed data by repeating it until this computed model is close enough to real model and error become very less. This scheme of model computation from observed data is called inverse modeling. In case of 1D structure, modeling and inversion is relatively simple than 2D and 3D. Linearized least square inversion and minimum norm inversion are the basic approaches for inversion. Various scheme of inversion are available which use these basic approaches with additional changes. There are number of software available perform inversion using different inversion scheme. MT2DInvMatlab is one of them which used for 2D inversion of magnetotelluric data. Detailed description of MT2DInvMatlab is given in following section.

4.1 MT2DInvMatlab Theory

MT2DInvMatlab is a software package for two dimensional inversion of magnetotelluric data. It is written in mixed language of MATLAB and FORTRAN. This program run in MATLAB environment so easily handled, and inversion process can be visualized. To reuse of exiting code and speed up computation some internal function are written in FORTRAN. MT2DInvMatlab use finite element method to compute 2D MT response of geological structure. In inversion process, smoothness-constrained least square inversion scheme used, by spatially variable regularization parameter algorithm. It also supports smooth varying topography.

4.1.1 Forward modeling

The governing equations for the TE and TM modes of MT fields can be written as

$$\nabla \left(\frac{1}{\tau} \nabla V \right) = \gamma V \quad 4.1$$

where $V = H_y$, $\gamma = i\omega\mu$, $\tau = \sigma$ for the TM mode, and

$V = E_y$, $\tau = i\omega\mu$, $\gamma = \sigma$ for the TE mode.

where σ is the conductivity of the earth, μ_0 is the magnetic permeability of the air ($4\pi \times 10^{-7}$ H/m), ω is the angular frequency of incident MT fields, and $i = \sqrt{-1}$.

Solution of equation (4.1) gives MT field V and for calculation of other MT parameters we need corresponding auxiliary fields I and J , which can be calculated by differentiation of MT field V with respect to x and z as:

$$\frac{\partial V}{\partial x} = -\tau I \quad 4.2.1$$

$$\frac{\partial V}{\partial z} = -\tau J \quad 4.2.2$$

Now impedances in TM and TE modes in terms of these auxiliary fields can be given as:

$$Z_{xy} = \frac{E_x}{H_y} = \frac{J}{V} \quad 4.3.1$$

$$Z_{yx} = \frac{E_y}{H_x} = -\frac{V}{J} \quad 4.3.2$$

Solution of equation (4.1) can be obtained using finite element method. Finite element formulation (Becker et al., 1981) of equation (4.1) using weighted residual method gives following integral equation:

$$\int_{\Omega} \frac{1}{\tau} \nabla U \nabla V \, dS + \int_{\Omega} \gamma UV \, dS = \int_{\partial\Omega} \frac{1}{\tau} U \frac{\partial V}{\partial n} \, dl \quad 4.4$$

where U is a test function, Ω is the domain, $\partial\Omega$ is the boundary of domain Ω , and n is the length of a vector n outward normal to boundary $\partial\Omega$. Dividing the whole computation domain Ω into finite elements Ω_e 's, and applying Galerkin approximation of equation (4.4) yield a basic equation for FE formulation over each element

$$\int_{\Omega_e} \frac{1}{\tau} \nabla N_i \nabla N_j \, dS + \int_{\Omega_e} \gamma N_i N_j \, dS = \int_{\partial\Omega_e} \frac{1}{\tau} N_i \frac{\partial V}{\partial n} \, dl \quad 4.5$$

where $\{N_i; i=1,2 \dots N_e\}$ are basis functions chosen for shape and test functions of the order N_e over an FE element, Ω_e represents an individual element in the FEM mesh, and $\partial\Omega_e$ is the circumference of element Ω_e . In implementation, linear functions used for shape and test functions, and therefore N_e equals 4.

Boundary conditions is used as suggested by Rodi (1976), according to it earth subsurface can be assumed as 1D layer structure at regions far from the 2D structure modeled. To satisfy this, additional elements were added in both side of the model, mathematically it can be written as:

$$\frac{\partial V}{\partial x} = 0 \quad 4.6$$

In the TM mode, at top surface earth material assume as non-magnetic which gives constant H_y at the surface. Additional elements were added on top of model to satisfy boundary conditions in air, which gives H_x in the air distant from the model, is constant as:

$$H_x = \frac{1}{i\omega\mu} \frac{\partial E_y}{\partial z} = \text{constant} \quad 4.7$$

Further, half-space impedance boundary conditions are applied at the bottom of the FE mesh as:

$$\frac{1}{\sigma} \frac{\partial H_y}{\partial z} + Z_H H_y = 0 \quad 4.8$$

for the TE mode,

$$\frac{1}{i\omega\mu} \frac{\partial E_y}{\partial z} + \frac{1}{Z_H} E_y = 0 \quad 4.9$$

In the program, additional enough blocks are added in the z direction to avoid 2D effect.

4.1.2 Least squares Inversion

Any forward problem can be present in following form:

$$d^m = A(m) \quad 4.10$$

Where A is a forward modeling operator generally nonlinear, m is a model parameter vector, and d^m is a model response vector. For real earth problem above equation is an ill posed inverse problem. It can be solved by minimization of Tikhonov parametric functional (Tikhonov and Arsenin, 1977),

$$P(m) = \phi(m) + \lambda^2 s(m) \quad 4.11$$

Where $\phi(m)$ is a misfit functional and $s(m)$ is a stabilizing functional and λ is a regularization parameter. λ control contribution of $\phi(m)$ and $s(m)$ in $P(m)$ in minimization. Misfit and stabilizing function are present as:

$$\phi(m) = \|d - A(m)\|^2 \quad 4.12$$

$$s(m) = \|Cm\|^2 \quad 4.13$$

Where C is a model parameter weighting matrix.

Smooth constrained least square inversion method used for solving this inverse problem.

Linearization of equation (4.10) and approximation gives:

$$\Delta m = (J^T J + \lambda^2 C^T C)^{-1} J^T \Delta d \quad 4.14$$

Where Δd is the error between the observed and the computed data, Δm is the modification in model parameter, J is the Jacobian matrix of forward modeling operator A, C is a laplacian (second order) smoothness operator (Scales et al., 2001).

On every computation of least square inversion, jacobian function is computed to calculate the modification in model parameter vector. In MT2DInvMatlab program reciprocity method is used to compute sensitivity function to make it efficient. During implementation, model parameters and input parameters are converted into logarithmic value to avoid negative value during inversion (Lee et al., 2009).

4.2 Files Description

MT2DInvmatlab program is code written in MATLAB and FORTRAN and run in MATLAB environment. MT2DInvMatlab needs three input files and create a figure, MAT file and an output file containing inversion results. First of three names listed below are input files and last one is output file:

1. Parameter script file (*.m)
2. Field Data File (*.FDT)
3. Topography File (*.TOP)
4. MT Inversion Result File (*.MIR)

4.2.1 Parameter script file (*.m): It is a MATLAB script file, has all parameters needs MT2DInvMatlab control inversion process. Descriptions of these parameters are given below:

- **DataFolder, ModelName, MTDataFileName, MTInvFileName, MTTopoFileName:** These parameters locate field data files, naming different variables, structures and file.
- **Mode(TM, TE, and Joint), PhaseIncluded, TopoIncluded, InversionMethod, No of Iterations, Lambda, LambdaMin, LambdaMax:** These parameters are related to inversion schemes. *Mode* can have value 1, 2 or 3 corresponding to TM, TE or joint mode respectively. *PhaseIncluded* and *TopoIncluded* can have value 1 or 0 depend on whether you want to use Phase and Topography data or not. *Lambda* is a regularization parameter and *LambdaMin* and *LambdaMax* gives range for it.
- **MaxDomainFactor, BlockIncFactor, SurfaceBlockThickness, BlockDivMethod, NoBlocksideX, NoBlocksideZ, NoCellPerBlockX, NoCellPerBlockZ:** These helps programme to design the meshgrid for finite element method. *MaxDomainFactor* limits depth of investigation. *MaxDomainFactor* times of maximum skin depth are the depth of mesh. *BlocIncFactor* decide increment in thickness of inversion block in z direction. *SurfaceBlockThickness* will be thickness of surface blocks. *NoBlocksideX* and *NoBlocksideZ* number add some more block in x and z direction.

NoCellPerBlockX and *NoCellPerBlockZ* make finer grid by dividing inversion block into more blocks.

4.2.2 Field Data File (*.FDT): Field Data file contain observed resistivity and phase component, Frequencies, Station location, and mode of inversion. Format of Field data file (*.FDT) is as:

#1: Header

#2: Mode (1= TM mode; 2=TE mode; 3= Joint inversion of TM and TE)

#3: The first coordinates of first MT station.

#4: The minimum spacing between MT stations.

#5: Number of stations and the number of frequencies

#6: The identifiers and positions of the MT stations

#7: The frequencies

#8: Apparent resistivity's and phases for all frequencies at all MT stations.

4.2.3 Topography File (*.TOP): Topography file has topography corresponding to each station. Topography data file is in the form of two column matrix data one have station location and another elevation started with the header @@@ TOPO.

4.2.4 Output MT inversion file (*.MIR): MT2DInvMatlab writes the inverted resistivity at each iteration stages together with the inversion control parameters which is given by parameter script file. It also have value of Minimum and Maximum Apparent resistivity, Logarithmic mean of apparent resistivity, Minimum and Maximum Skin depth, Data Misfit, Coordinates of inversion blocks.

MT2DInvMatlab programme save all variables of inversion as in standard MAT files so that users can check in the raw format. After completion of iteration, it gives final figure showing observed and modelled pseudo sections and 2D resistivity section of subsurface beneath stations.

4.3 Data Editing

Basics theory of MT2DInvMatlab program have discussed and also data acquisition and processing of acquired data are described in previous chapters. Input .FDT file created from these processed data by arranging them in proper format so it can be used in

MT2DInvMatlab program. Before arranging in proper format, good quality data selected. Since, we have data at 42 stations and geographic map of those station were shown in figure (2.1). Many stations are very close to each other and in these some of them have good quality data and some have bad quality. So averaging of data for close stations was performed to remove cluster of station. Closed stations data are averaged to one station data. Averaging was done on basis of weight of error or spacing, or median of data.

Averaging based on spacing: Select reference station (which has good data quality) from group of stations. Compute relative spacing of each station from reference station. Inverse of relative spacing is weight given to each station data. If weight is greater than unit then keep it to unit value. Averaging was done by following formulae:

$$d_{av} = \frac{\left(\frac{d_1}{r_1} + \frac{d_2}{r_2} + \dots + \frac{d_n}{r_n}\right)}{\left(\frac{1}{r_1} + \frac{1}{r_2} + \dots + \frac{1}{r_n}\right)} \quad 4.15$$

Where d_1, d_2, \dots, d_n are data at n^{th} station and r_1, r_2, \dots, r_n are corresponding relative spacing from reference station.

Averaging based on error: In this averaging, weight is inverse of data error corresponding to each data. Reference site was used only for referring location of averaged data. A formula for this scheme is similar as equation (4.15) where d 's are data value but r 's will be corresponding error value.

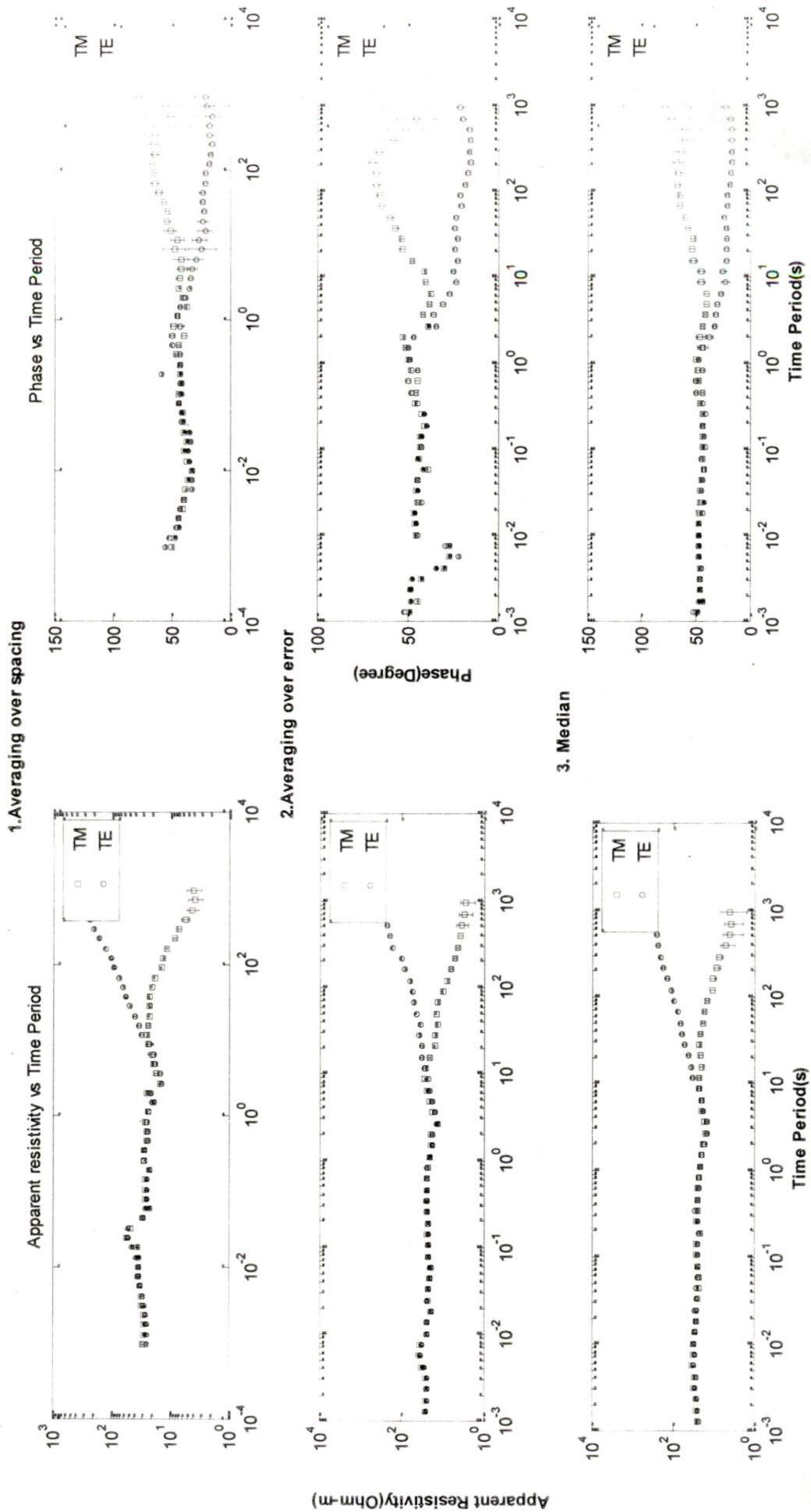
Median: In this scheme, median of all data is taken of group at each frequency, and reference site will be the location for averaged data.

Group of station that are averaged, and their reference site are listed in table (4.1).

Table 4.1: List of averaged Stations and corresponding reference Station.

S.No.	Group of Stations	Reference Site
1	1,2,3,4	2
2	6,7,8,9	6
3	10,11,12	11
4	13,14,15,16	15
5	18,19,20	18
6	24,25,26	25
7	27,29,31	27
8	32,34	34
9	43,44	44
10	48,50	48

Figure 4.1 Plot of averaged apparent resistivity and phase for group 1



Plot of averaged data for each method for group no. 1 are shown in figure (4.1). We see that median scheme showing more smoothness than other method.

Since some data are recorded by Phoenix system and they are processed by different software so they have difference frequencies number. Spline interpolation is used to calculate data at required frequency value.

Finally, after averaging and interpolation of data, 18 station data were selected for using input data in inversion program. Map of these 18 stations created by GMT with the help of MR. Suresh Kanuajiya, is shown in Figure (4.2).

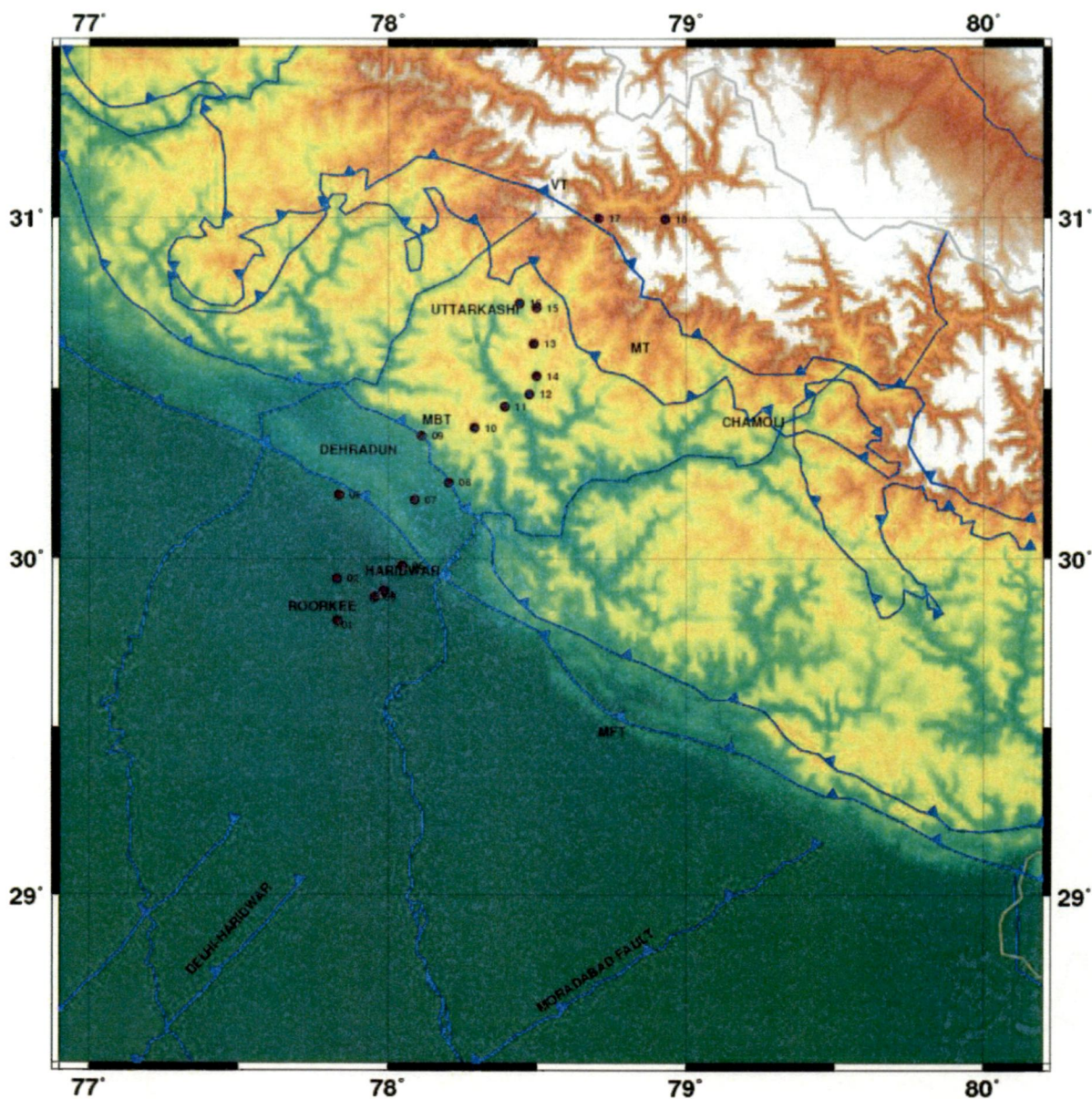


Figure 4.2 Map of 18 Station

CHAPTER 5

RESULT AND DISCUSSION

5.1 Inversion of field Data

After processing and averaging of the 42 MT sites data recorded along Roorkee-Gangotri profile, only 18 sites were selected for 2D inversion. Sites were projected to profile line which cross the major Himalayan thrusts: Himalayan Frontal Thrust (HFT), Main Boundary Thrust (MBT) and Main Central Thrust (MCT). Removed sites have highly noisy data and phase exceeding 90° . The selected 18 sites data were rotated $N30^{\circ}E$ in the direction of strike direction. In order to reducing 3D effect and strike deviation, penalties applied in error bars. The inversion is carried out for three modes: TE-, TM-, joint inversion of TE, TM modes. Results of joint mode are not good and satisfactory so it not discussed here.

MT2DInvMatlab start inversion process with many calculations like minimum, maximum and mean apparent resistivity and skin depth. Mean of apparent resistivity is used as an initial value for inversion.

MT2DInvMatlab software package comes with sample data files, so anyone can run and learn it. I successfully run program for sample data file and it produce same result as it required. Then 14 station data with 47 frequencies were used to run program. But result produced by this has very high resistivity in range of 10^{10} - 10^{20} . And also program run only for TM mode. MT2DInvMatlab program used input resistivity and phase in logarithmic value to avoid negative value in inversion. Since TM mode have phase in range of 0 to 90. But TE mode phase are in third quadrant and it represent in negative numbers. This is reason why program is not executing for TE and Joint mode and giving high resistivity value. So this problem was resolved by converting TE mode phase value from third quadrant to first quadrant by adding 180 degree.

For execution of program, FORTRAN compiler should be installed in your computer, because MT2DInvMatlab program run in MATLAB environment but it is written in mixed language MATLAB and FORTRAN. Also for higher version of MATLAB like 2010a and it runs smoothly.

Further, I used 35 station data for inversion; it takes very long time in execution and results is also not good. So we observe that there are many clusters of stations, among any clusters some station have good data and some are noisier. We take average of them to remove crowd of station and reduce the effect of noisy data. Since we have two type data (Phoenix and

Metronic) and frequency range and frequencies of data are different in both case. So we use interpolation on Phoenix data to match frequencies to data recorded by Metronics system. To match frequencies, we have to remove some frequencies data from Metronics data and thus we have total 18 stations and 24 frequencies give profile of 170 km. Finally these data were used for inversion process and their result is shown and discussed in next section.

5.2 Results and Discussion

18 stations data having 24 frequencies with topography is used for inversion. Parameters set in parameter script file are as follows:

PhaseIncluded: Yes (=1),
TopoIncluded: Yes (=1),
InversionMethod: Second order constrained (=2),
Iteration: 10,
MaxDomainFactor: 0.2 (limiting depth to 50 km),
BlockIncFactor: 1.0
SurfaceBlockThickness: 40
NoBlockSideX and NoBlockSideZ: 0 (not to add addition block in X and Z direction)
BlockDivMethod: 0 for TE mode and 1 for TM mode)

Rest of other parameter was used as default. All these parameter are same for each mode. Distance between first and last station is 166 km. 2D Model generated by inversion have length 170 km, while depth of section is bounded to 50 km. Each station has data at 24 frequencies. Inversion section shows resistivity with JET color scale, where high resistive body is shown by blue color and conductive body by red color. Resistivity increases in scale from red to yellow to green to blue color.

Result of TE and TM mode good and fit with geological features of area, but Joint mode result is not good so it not presented here. For TM and TE mode, pseudo section of calculated and observed resistivity and phase, and resistivity section is generated by program.

Figure 5.1 Pseudo Section of apparent resistivity and phase

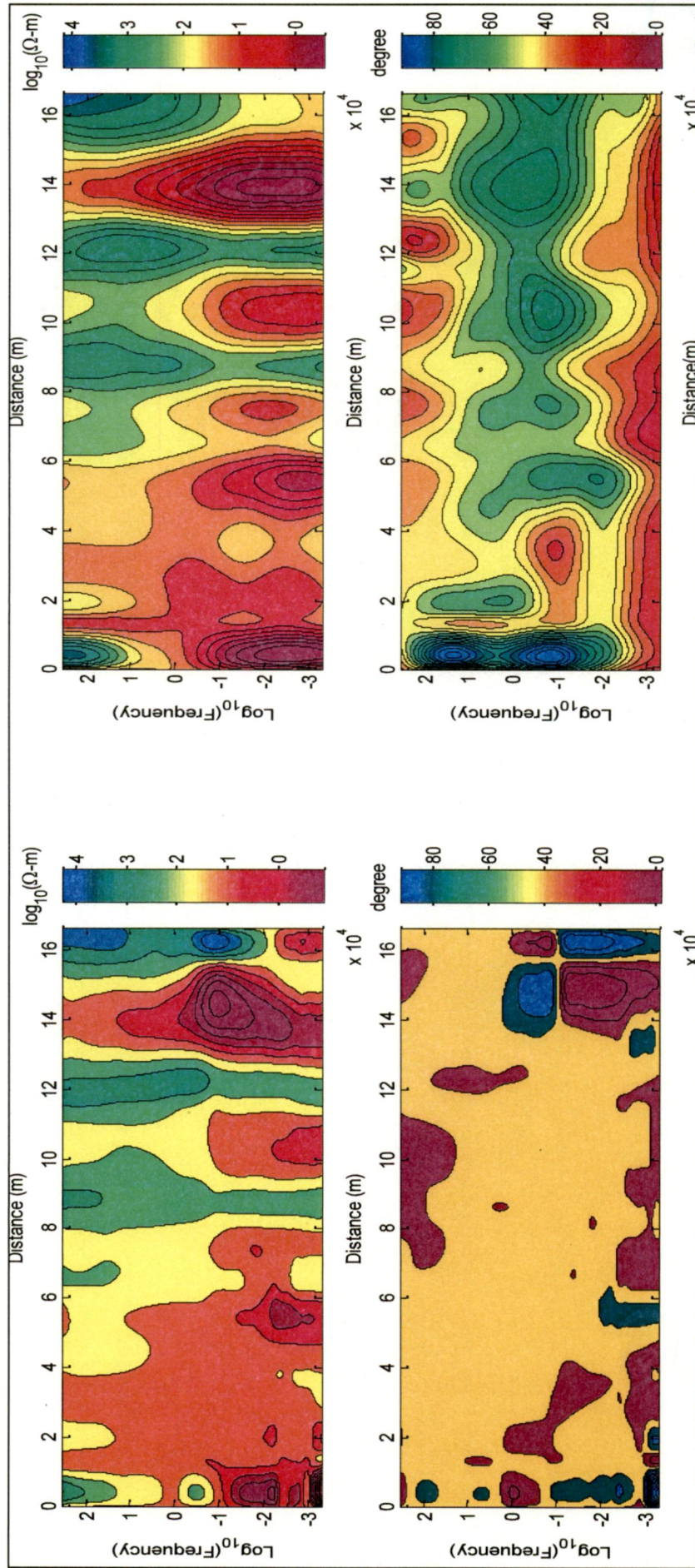


Figure 5.1.1 TM Mode

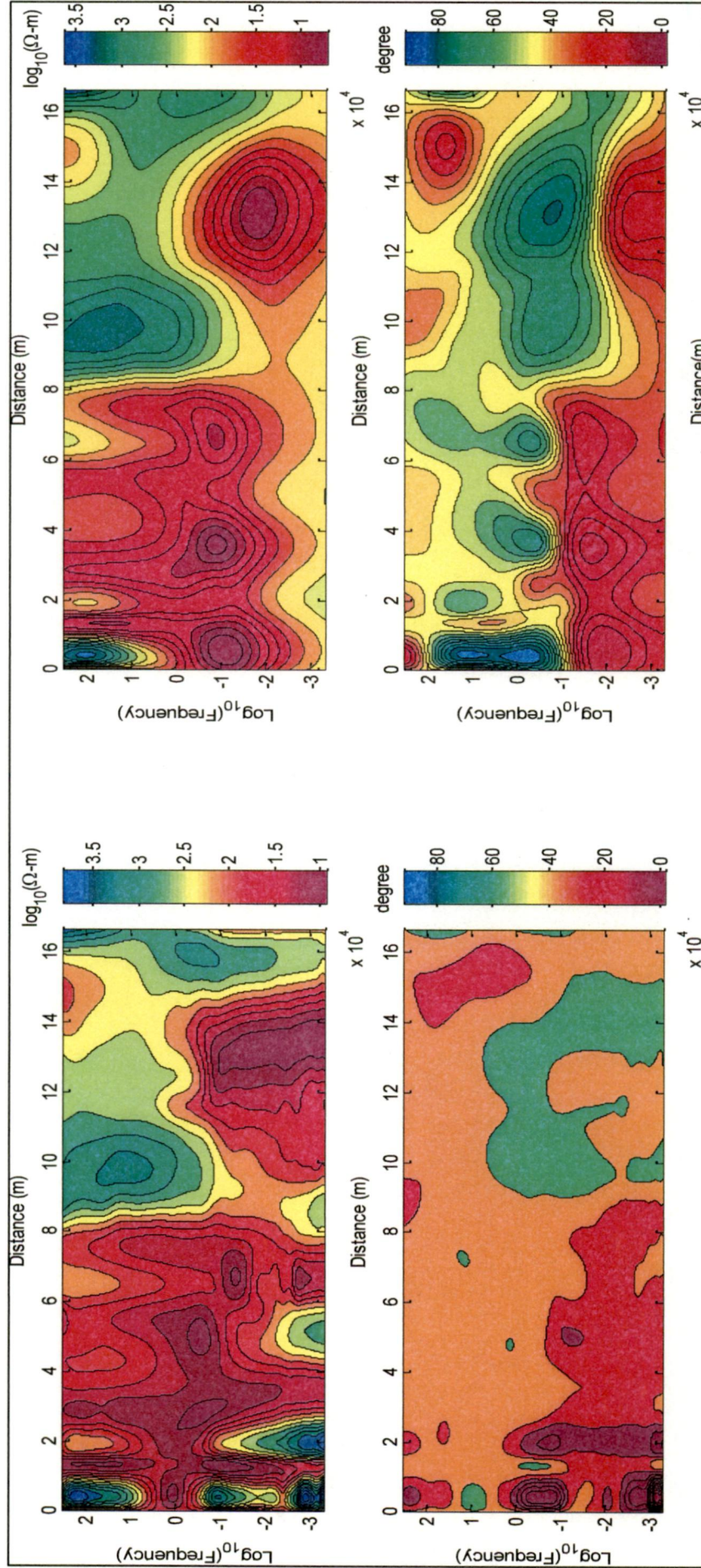


Figure 5.1.2 TE Mode

Inverted section for TM and TE mode is shown in figure (5.2). Calculated and observed apparent resistivity and phase is plotted on same graph to show the fitting. Figure (5.3) are plot of apparent resistivity and phase for TM mode and Figure (5.4) are plot of apparent resistivity and phase for TE mode.

In Israil et al., 2008 carried out MT survey for electrical structure along same profile. Figure (5.2.3) (M. Israil et al., 2008) showed resistive section beneath Roorkee-Gangotri profile having different electrical structure, coincidence with intense micro seismic activity and the position of the Himalayan major thrust. Figure (5.2.1) and (5.2.2) shows our resistivity model derived from the 2D inversion.

Figure 5.2 Models for TE and TM mode inversion

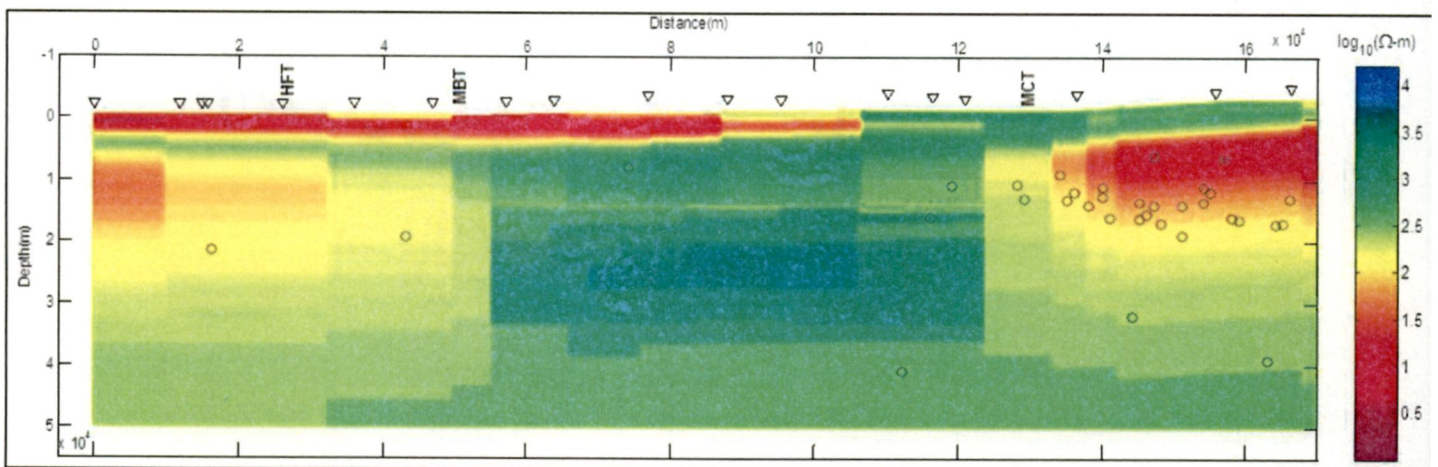


Figure 5.2.1 Model for TM Mode

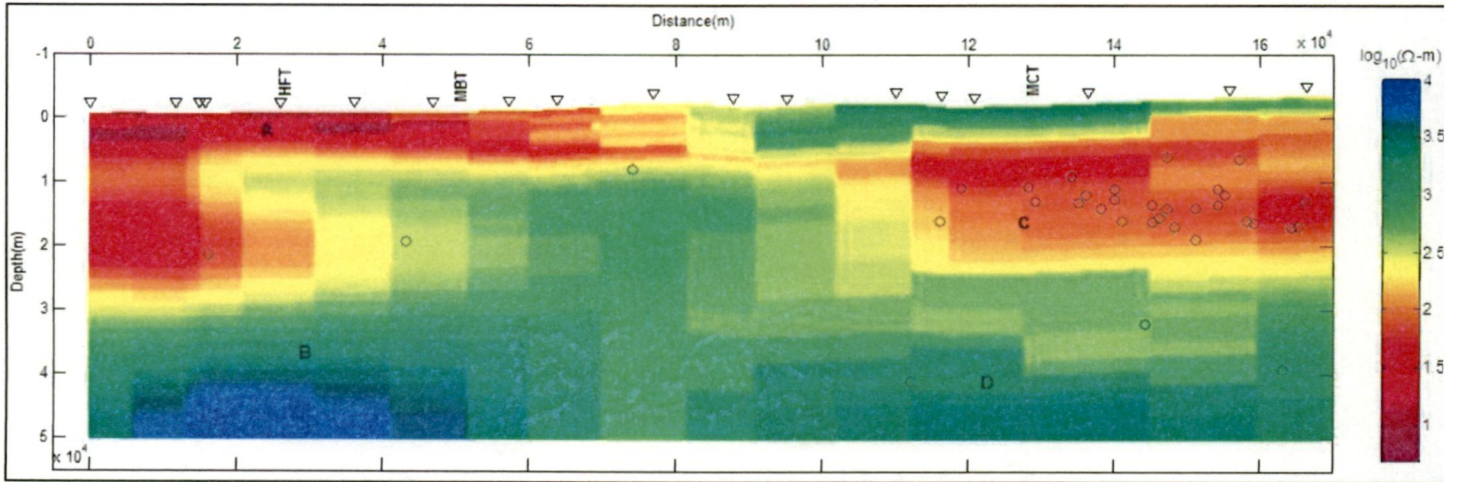


Figure 5.2.2 Model for TE Mode

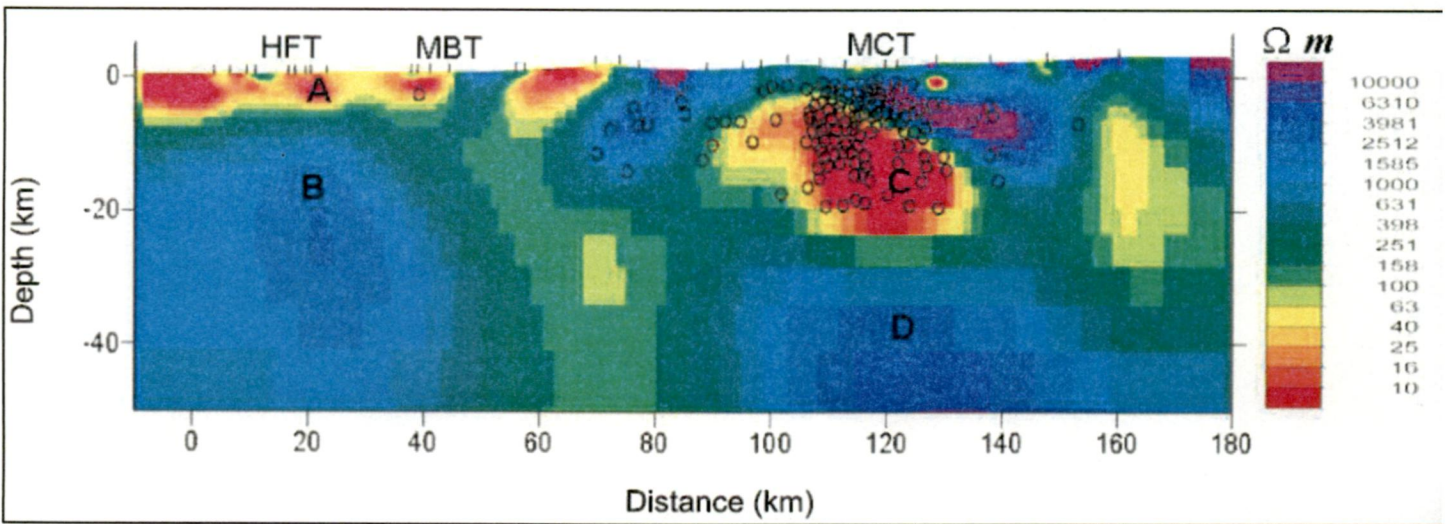


Figure 5.2.3 Model by Israil et al., 2008

Figure 5.3 Fitting plot for TM mode

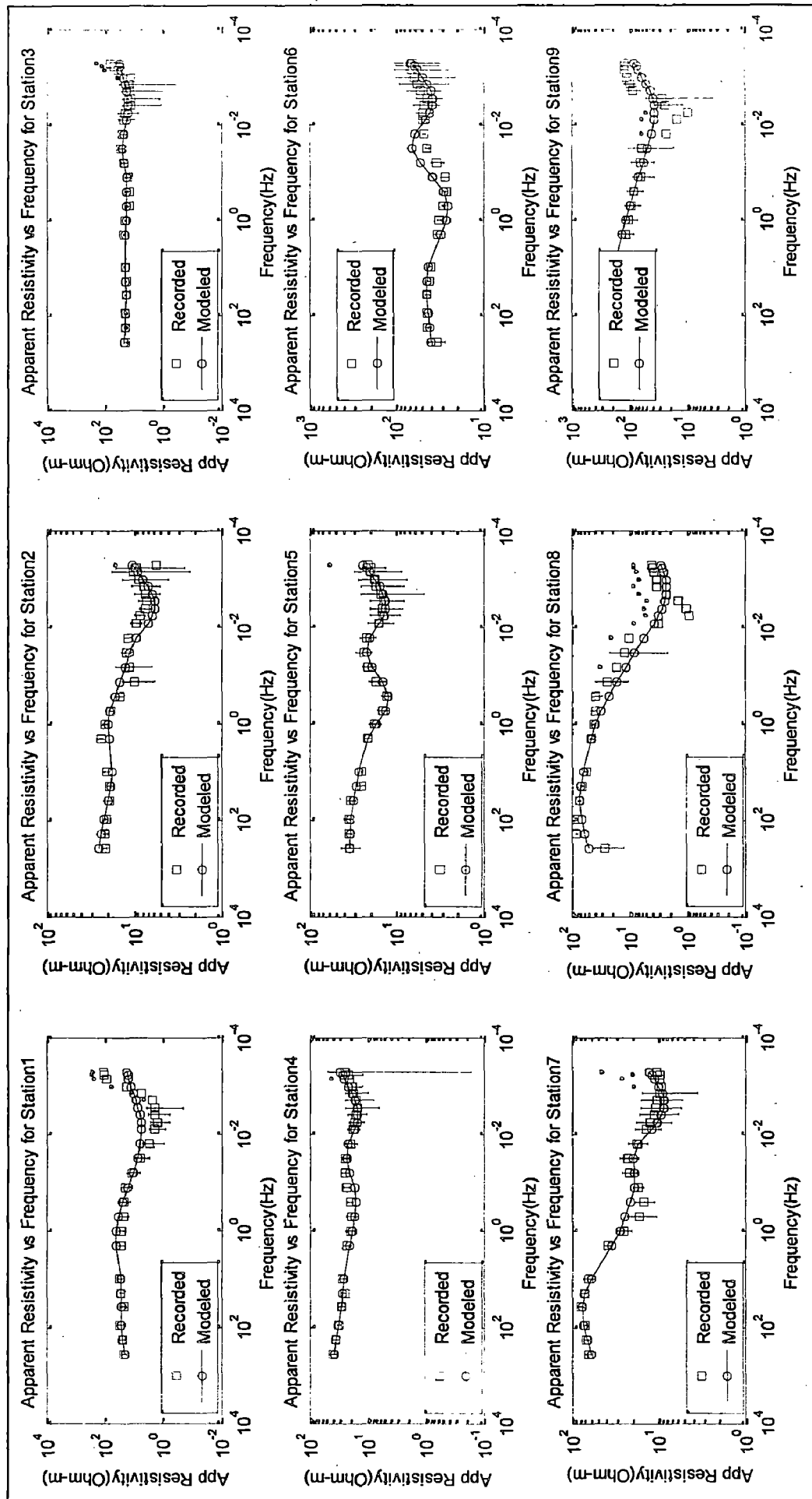


Figure 5.3.1 Resistivity fitting plot for TM mode (cont.)

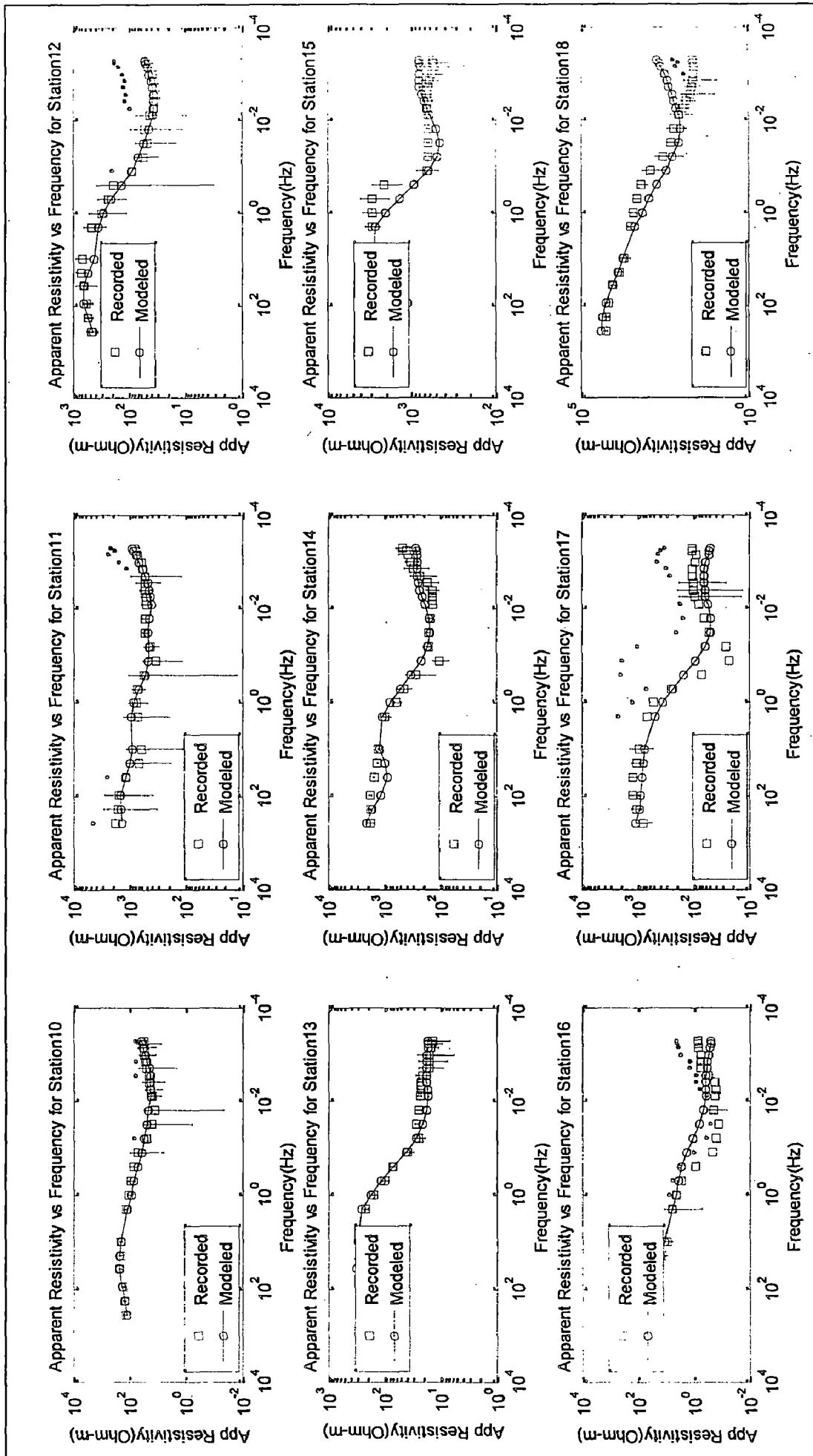


Figure 5.3.1 Resistivity fitting plot for TM mode

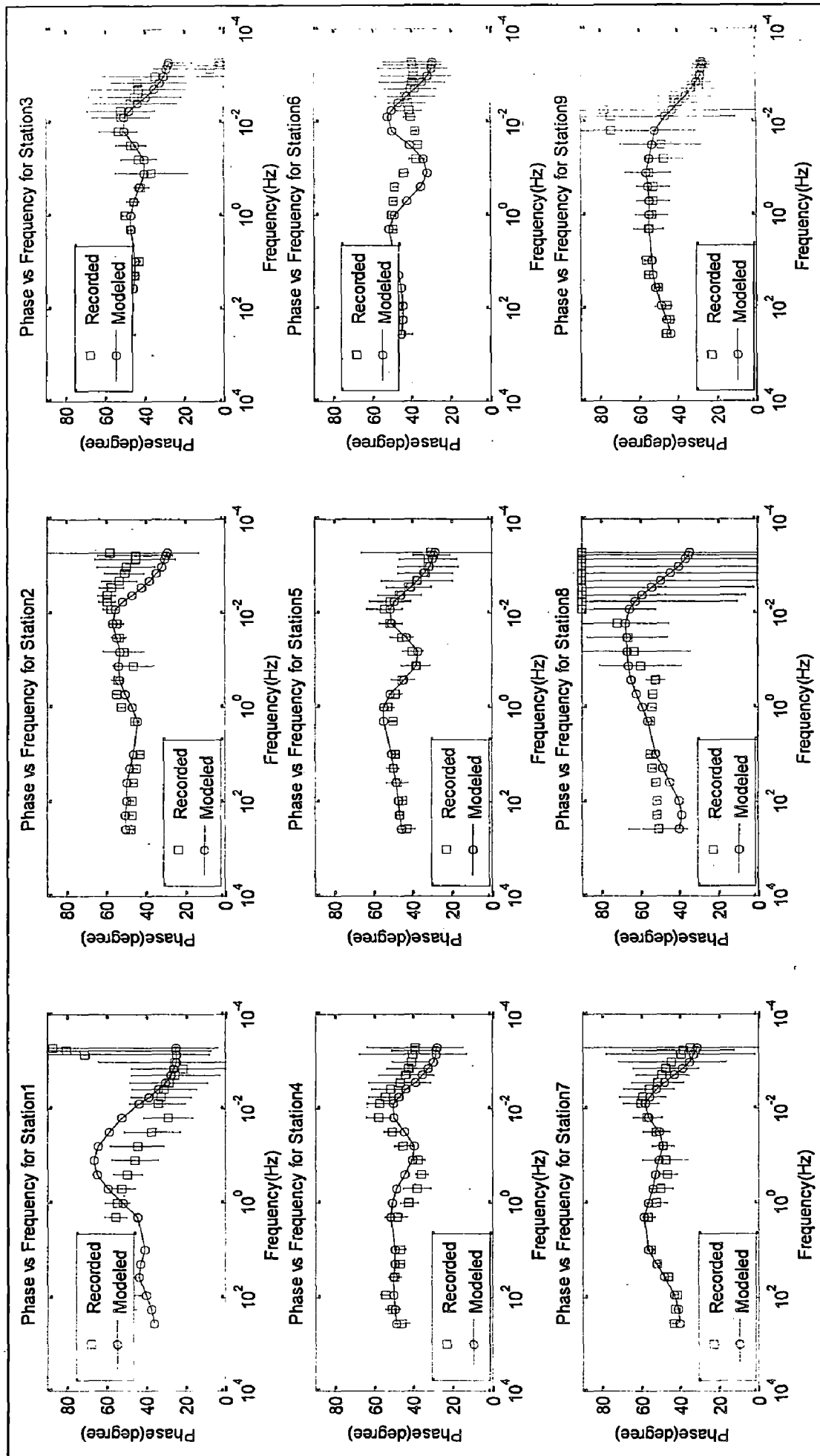


Figure 5.3.2 Phase fitting plot for TM mode (cont.)

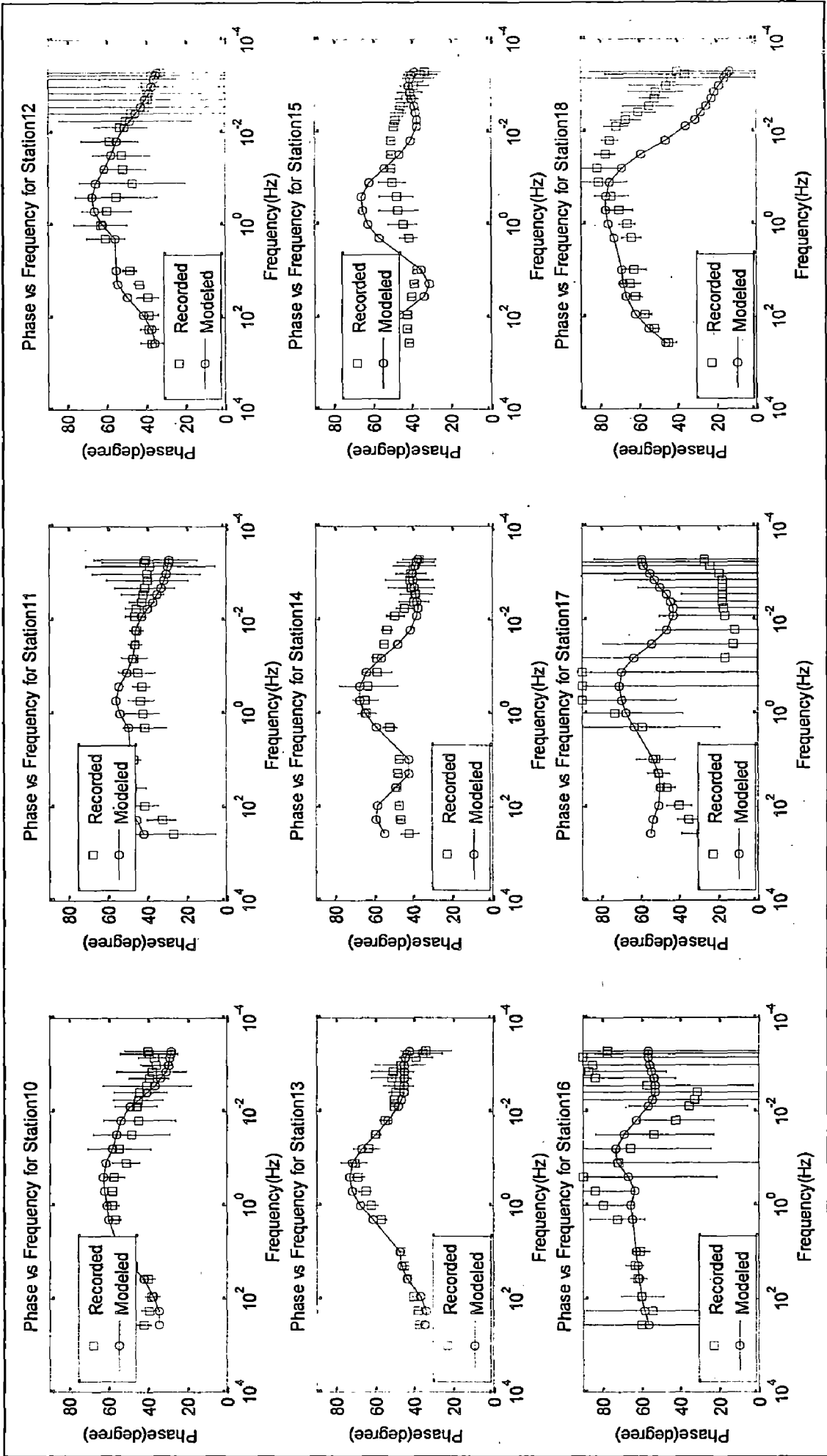


Figure 5.3.2 Phase fitting plot for TM mode

Figure 5.4 Fitting plot for TE Mode

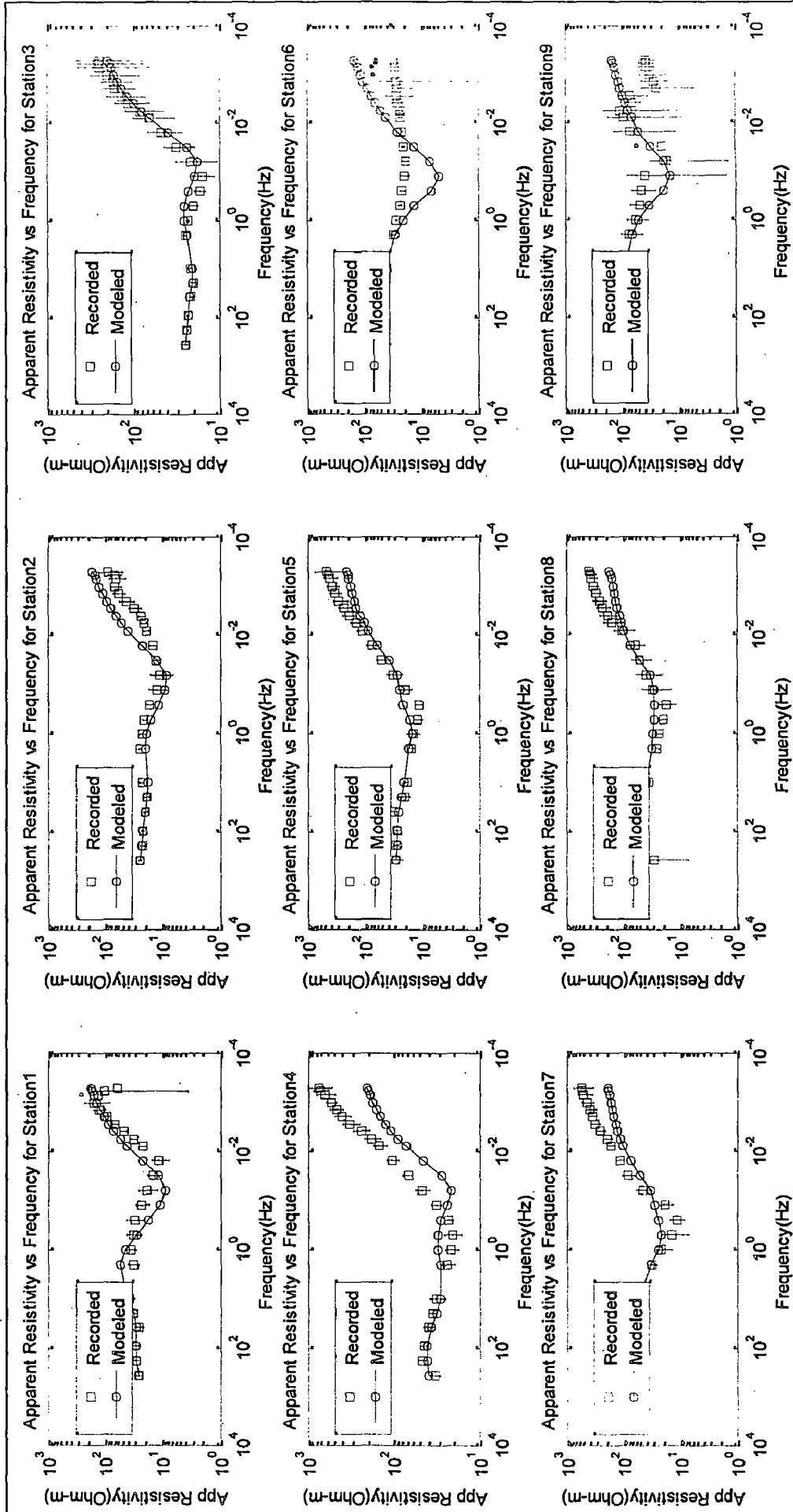


Figure 5.4.1 Resistivity fitting plot for TE mode (cont.)

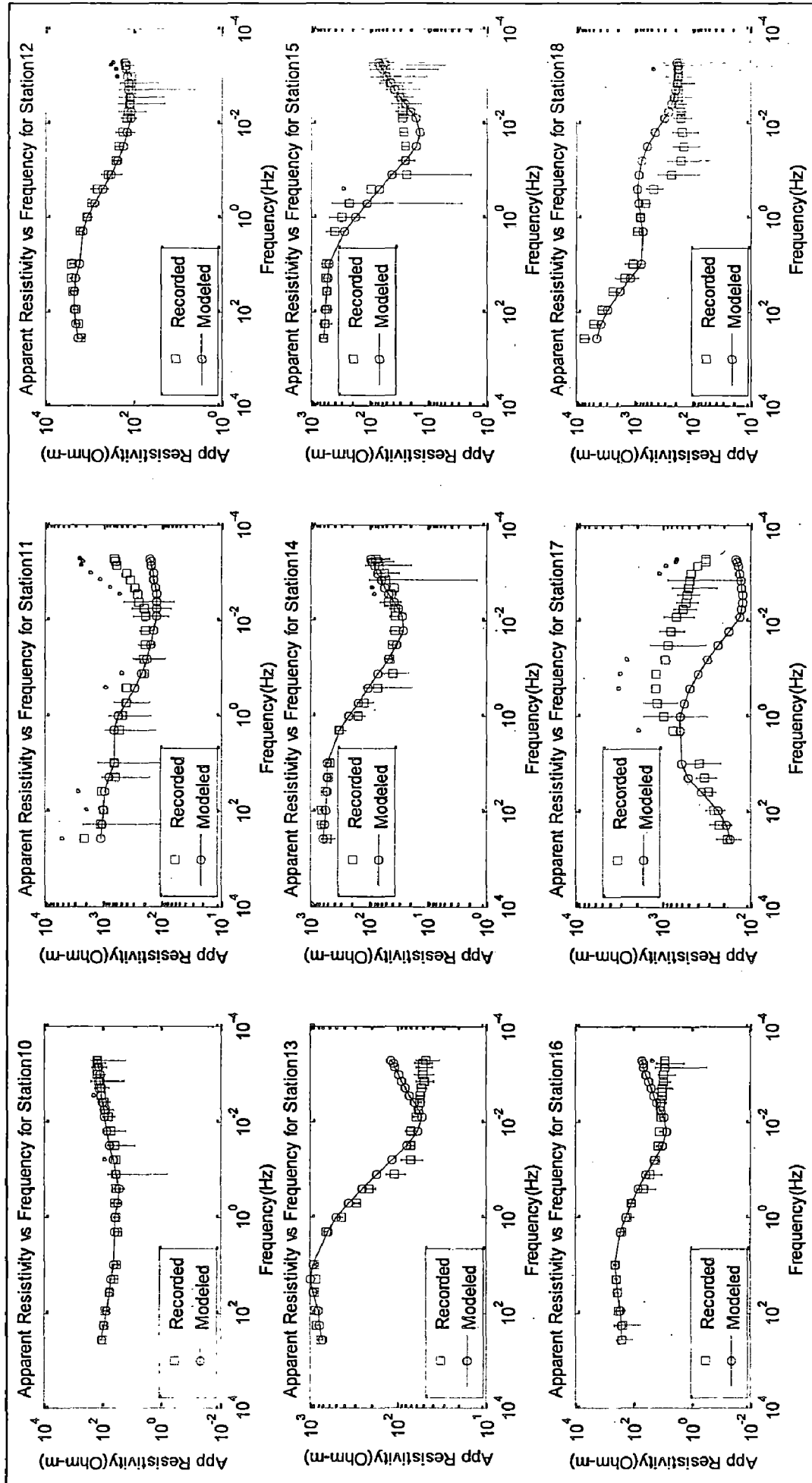


Figure 5.4.1 Resistivity fitting plot for TE mode

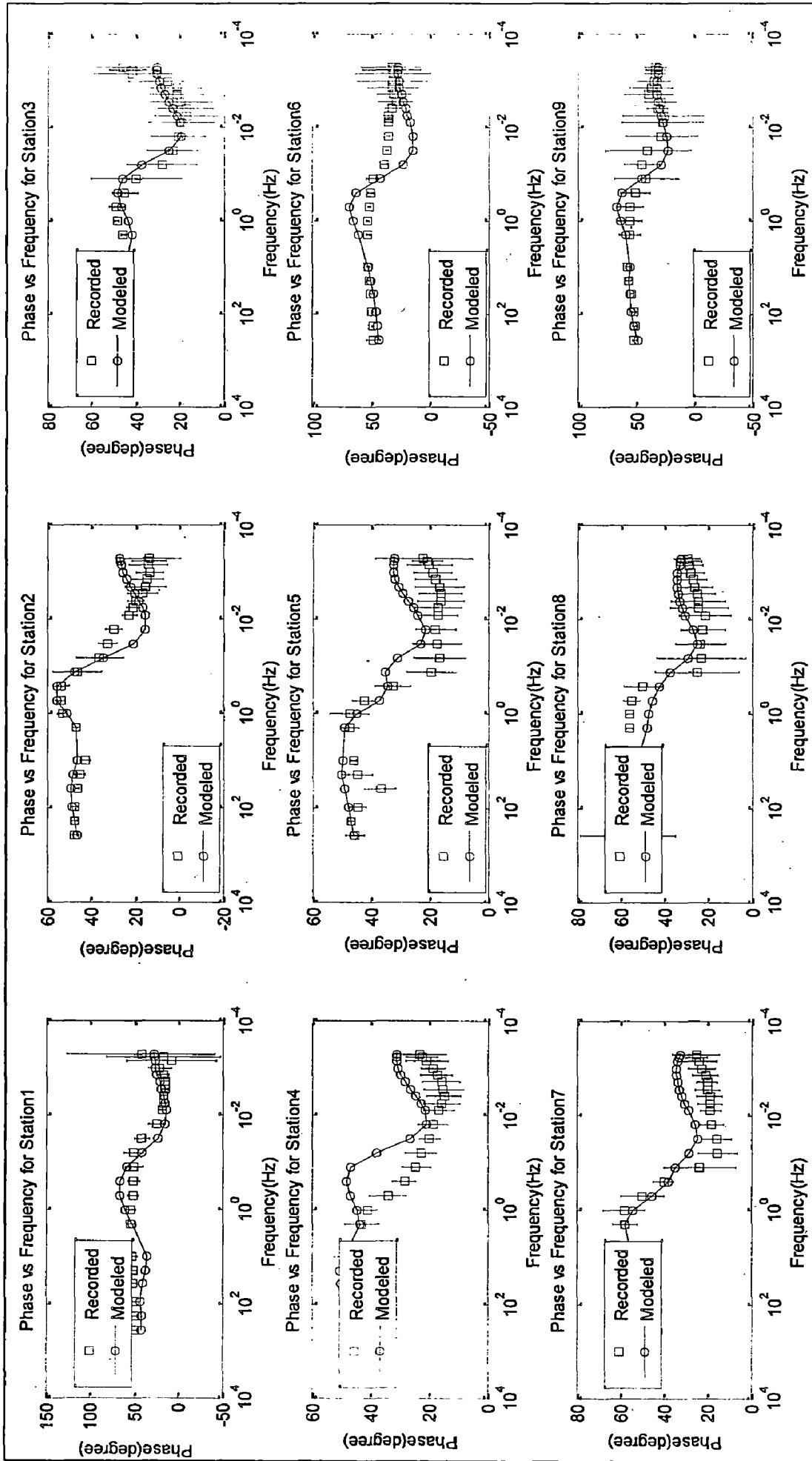


Figure 5.4.2 Phase fitting plot for TE mode (cont.)

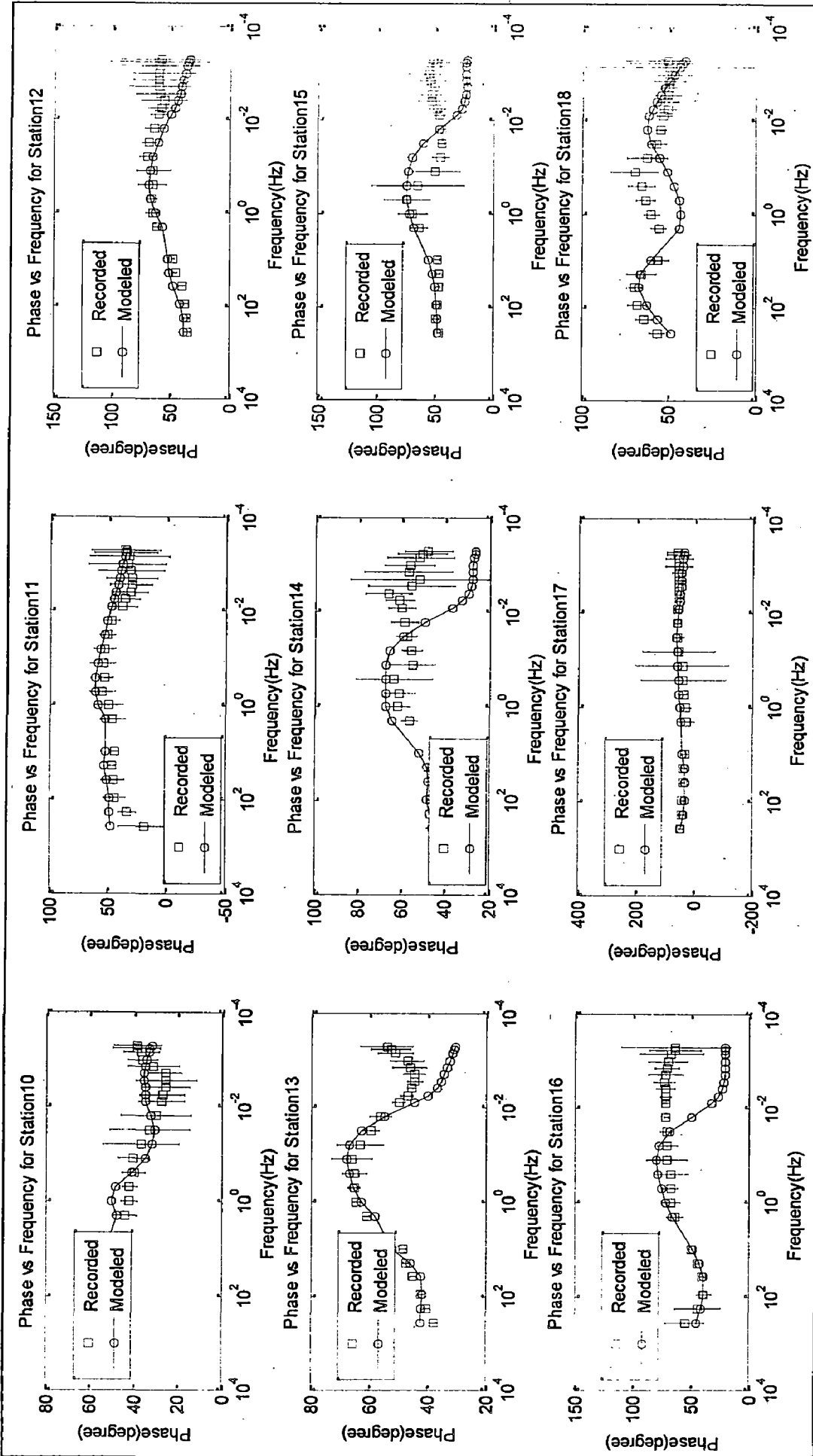


Figure 5.4.2 Phase fitting plot for TE mode

Above figures show pseudo section, inverted resistive section and fitting curves. We can see that all calculated pseudo section and fitting curves shows good match with corresponding observed plot. Fitting of resistivity and phase are shown for all 18 stations. These fitting curves for all station shows good fitting for higher frequencies, but for low frequency fitting are not good.

In the magnetotelluric (MT) survey, the inhomogeneous mediums underground make polarization apparent resistivity curve with TE and TM modes of measured data different. Therefore, different modes can get different interpretation results which will bring difficulty to understand and judge geologic configuration. TE mode has good vertical resolution whereas TM mode has horizontal resolution. Resistive section for each TM and TE mode are not exact same but they are showing similarity. TE model is indicated by four different zones: A, B, C, and D zones. Features of each zone are discussed below:

Zone A: This zone extends from 1 to 6 sites which are approximately 50 km long. It is a conductive structure in shallow depth of 6 km. Resistivity of zone A is less than 50 Ωm . This part located between Indo Gangetic plane and Lower Himalaya. This part has loose sediments which have age of Miocene and younger age, it formed by sediment transformed from Higher Himalayan region. Below this conductive zone, there is resistive zone which is the top of Indian plate. So, Zone A is an important electrical structure, which located on the top surface of the Indian plate.

Zone B: Zone B is a resistive zone, which have resistivity larger than 1000 Ωm . It's lie below the conductive sediments of shallow depth. It extended from 30km to 50 km. Maximum resistivity of this zone is very high (>6000 Ωm). It is interpreted as an electrical image of the Indian crust.

Zone C: This is also a conductive zone having low resistivity (<50 Ωm), which present beneath MCT and extended from Lesser Himalayan to Higher Himalayan laterally. Along profile, it extends laterally from 110 to 160-170 km having depth 5 to 25 km. It is a typical example of conductive zone in mid crustal region observed in the Himalayan region.

Hypocenters of local earthquake coincide with zone C (Rai S.S., 2012). Main Central Thrust (MCT) zone exhibits high heat flow area where numbers of hot springs are concentrated around this zone. It has been reported by GSI (1991) that it has high heat flow (130 \pm 30mW/m²) and high temperature gradient (60° \pm 20° C/km). While foot hill

Himalayan belts exhibit low heat flow ($41 \pm 10 \text{ mW/m}^2$) and low temperature gradient ($17^\circ \pm 5^\circ \text{ C/km}$). On the account of a foresaid fact it has been proposed that the subsurface temperature is increased in the MCT zone and the probable source of high heat flow is partial melt associated with fluids. This zone is demarked by a low resistivity value. It interpreted as a partially molten layer and the zones of high heat flow in MCT zone. The most probable conductive phase is fluids (Lemonnier *et al* 1999).

Zone D: This is a resistive feature underlying the low resistivity zone in mid crustal depth. Resistivity of this zone appears to be affected by the low resistivity zone on top of it. We interpret this feature as electrical image of the Indian crust.

TM model have also these zones but resistivity is comparatively less than TE mode. For example corresponding to Zone A, it also have shallow conductive zone extended from 1 to 11 site of length 85 km. Depth of this shallow conductive body is 4 km.

A model along same profile from Israil *et al*, 2008, is shown in figure (5.2.3). This model also shows the zone A, B, C, and D. In this model local earthquake hypocenter location were taken from Khattri, 1992. We can see that our model show very similarity with this model (Israil, 2008). But in my model, zone C is extended up to 160-170 km along profile and it exactly coincide with location of local earthquake hypocenters given by Rai, 2012.

CHAPTER 6

SUMMARY AND CONCLUSION

MT acquisition was done along profile passes through hills and valley type topography from Roorkee to Gangotri at 42 stations. MT data were acquired using Metronix MT system and Phoenix System. The acquired time domain MT data were processed using MAPROS, SSMT 2000 and PRC-MTMV software. To avoid cluster of stations, data from group of stations were averaged. Overall 18 station data were selected. 2D smooth constrained least square inversions were carried out for the selected data set for an average strike angle of N30⁰E. Following conclusions were made from the resulted resistive section:

- (i) A near surface shallow conductive zone extends from 1 to 6 sites which are approximately 50 km long. This conductive zone vertically extends to 6 km. It lies in Indo-Gangetic Plane and Lesser Himalaya region.
- (ii) Highly resistive Indian basement is present beneath of shallow conductive zone.
- (iii) A conducting zone appears in the vicinity of MCT at depth of 10 km, which extended up to 20 km. This is a typical example of mid crustal conductor and overlap with the intense microseismic activity in the region.

Finally, geoelectrical model is interpreted to the possible geological and tectonic features along the profile. Shallow conductive zone is related to the molassic sediments, which transported from Higher Himalayan region. There is conducting zone which is seismically active and related with the strain accumulation zone in Himalayan region. This geoelectrical model is in good comparison with the model along same profile given by Israil et al, 2008.

All attempts were made to find a geologically acceptable model based on 2D inversion of MT data along Roorkee-Gangotri profile. It can be further improved by adding more data of better quality and using 3D inversion.

REFERENCE

- Akasofu S. I. and Kamide Y., "The Solar Wind and the Earth", Terra Scientific Publishing Company (TERRAPUB), Tokyo, 1987, pp. 73-100.
- Becker, E.B., Carey, G.F., Oden, J.T., "Finite Elements: An Introduction", Prentice-Hall Inc., Englewood Cliffs, NJ, 1981, pp. 255
- Cagniard L., "Basic Theory of the Magnetotelluric method of Geophysical prospecting, Geophysics, Vol. 18, 1953, pp. 605-635.
- Christopherson K. R., "MT Gauge Earth's Electric Field", AAPG Explorer, 1998, pp. 22-31.
- Christoffel D.A. and Linford J.G., "The Magnetotelluric method for locating major Geological Features and its application in the Wairarapa", New Zealand Journal of Geology and geophysics, Vol. 11, No. 1, 1968, pp. 66-77.
- Ernst T., Sokolova E.Y., Varentsova I. M., and Golubev N. G., "Comparison of two techniques for magnetotelluric data processing using synthetic data sets, Acta Geophysica Polonica, Vol. 49, No. 2, 2001, pp. 213-243.
- "Data Processing User Guide", Version 3.0, July 2005.
- Gamble T.D., Goumbau W.M., and Clark J., "Error Analysis for Remote Reference Magnetotellurics", Geophysics, Vol. 44, 1979b, pp. 959-968.
- "Geothermal Atlas of India", Geological Survey of India, Special Publication, Vol. 19, 1991.
- Israil M., Tyagi D. K., Gupta P. K. and Sri Niwas, "Magnetotelluric investigations for imaging electrical structure of Garhwal Himalayan corridor, Uttarakhand, India", J. Earth Syst. Sci. 117, No. 3, June 2008, pp. 189-200.
- Jacobs J. A., Kato Y., Matshita S., and Troitskaya V. A., "Classification of Geomagnetic Micropulsations", Journal of Geophysical Research, Vol. 69, No. 1, 1964, pp. 180-181.

- Jones A. G., “Magnetotelluric data processing and Analysis”, MT Short Course, SEG 2002.
- Kaufman, A. A. and Keller G.V., “The Magnetotelluric sounding method”, Elsevier Scientific Pub. Co., New York, 1981, pp. 1-595.
- Khattri K. N., “Local seismic investigations in the Garhwal-Kumaun Himalaya”; Geol. Soc. India Memoir, Vol. 23, 1992, pp. 45–66.
- Lee S. K., Kim H. J., Song Y., Lee C. K., “MT2DInvMatlab—A program in MATLAB and FORTRAN for two-dimensional magnetotelluric inversion”, Computers & Geosciences, Vol. 35 (2009), pp. 1722–1734.
- Lemonnier C., Marquis G., Perrier F., Avouac J. P., Chitrakar G., Kafle B., Sapkota S., Gautam U., Tiwari D. and Bano M., “Electrical structure of the Himalaya of central Nepal: high conductivity around the midcrustal ramp along the MHT”; Geophys. Res. Let., Vol. 26, 1999, pp.3261–3264.
- Rai S.S., Mahesh P., Sivaram K., Paul A., Gupta S., Sarma R., and Gaur V.K., “One dimensional reference velocity model and precise locations of earthquake hypocenters in the central (Kumaon-Garhwal) Himalaya, 2012 (Pri-print).
- Rodi W. L., “A technique for improving the accuracy of finite element solutions for magnetotelluric data”, Geophysical Journal of the Royal Astronomical Society, 1976, Vol. 44, 483–506.
- Scales J. N., Smith M. L., and Treitel S., “Introductory Geophysical Inverse Theory”, Samizdat Press, USA, 2001, pp. 151-182.
- Semenov V. Yu., Obrabotka dannyykh MT zondirovaniya (Processing of MT Soundings), Moscow, 1985.
- Simpson F. and Bahr K., “Practical Magnetotelluric”, Cambridge University Press, U.K., 2005, pp. 1-78.
- Tikhonov A. N. and Arsenin V. Y., “Solutions of ill-posed problems” (V H Winston & Sons.), 1977.
- “V5 System 2000 MTU/MTU-A User Guide”, Version 1.6, September 2005.

- Varentsov Iv. M., Sokolova E. Yu., Martanus E. R., Nalivaiko K. V., and the BEAR Working Group, “System of Electromagnetic Field Transfer Operators for the BEAR Array of Simultaneous Soundings: Methods and Results”, *Izvestiya, Physics of the Solid Earth*, Vol. 39, No. 2, 2003, pp. 118–148, Translated from *Fizika Zemli*, No. 2, 2003, pp. 30–61.
- Vozoff K., Kerr D., Moore R.F., Jupp D.L.B., and Lewis R.J.G., “Murray Basin Magnetotelluric study”, *Journal of the Geological Society of Australia*, Vol. 22, No. 3, 1975, pp. 361-375.
- Vozoff K., “Model study for the proposed magnetotelluric (MT) traverse in north India”; *Tectonophys.*, Vol. 105, 1984, pp. 399–411.
- Weight D. E., “The SEG standard for Magnetotelluric data”, *Society of Exploration Geophysicists Annual Meeting*, 1988.
- Zonge K. L., and Hughes L. J., “Controlled Source Audio-frequency Magnetotelluric”, in *Electromagnetic methods in Applied Geophysics*, ed. Nabighian M. N., Vol. 2, *Society of Exploration Geophysicists*, 1991, pp. 713-809.